

Stress and Strain Propagation in Soft Viscoelastic Tissue

While Tracking Microscale Targets

by

Shahrzad Talebianmoghaddam

A Thesis Presented in Partial Fulfillment
of the Requirements for the Degree
Master of Science

Approved November 2015 by the
Graduate Supervisory Committee:

Jitendran Muthuswamy, Chair
Christopher Buneo
Bruce Towe

ARIZONA STATE UNIVERSITY

December 2015

ABSTRACT

Tracking microscale targets in soft tissue using implantable probes is important in clinical applications such as neurosurgery, chemotherapy and in neurophysiological application such as brain monitoring. In most of these applications, such tracking is done with visual feedback involving some imaging modality that helps localization of the targets through images that are co-registered with stereotaxic coordinates. However, there are applications in brain monitoring where precision targeting of microscale targets such as single neurons need to be done in the absence of such visual feedback. In all of the above mentioned applications, it is important to understand the dynamics of mechanical stress and strain induced by the movement of implantable, often microscale probes in soft viscoelastic tissue. Propagation of such stresses and strains induce inaccuracies in positioning if they are not adequately compensated. The aim of this research is to quantitatively assess (a) the lateral propagation of stress and (b) the spatio-temporal distribution of strain induced by the movement of microscale probes in soft viscoelastic tissue. Using agarose hydrogel and a silicone derivative as two different bench-top models of brain tissue, stress propagation was measured during movement of microscale probes using a sensitive load cell. I further used a solution of microscale beads and the silicone derivative to quantitatively map the strain fields using video microscopy. The above measurements were done under two different types of microelectrode movement – first, a unidirectional movement and second, a bidirectional (inch-worm like) movement both of 30 μm step-size with 3min inter-movement interval. Results indicate movements of microscale probes can induce significant stresses as far as 500 μm laterally from the

location of the probe. Strain fields indicate significantly high levels of displacements (in the order of 100 μm) within 100 μm laterally from the surface of the probes. The above measurements will allow us to build precise mechanical models of soft tissue and compensators that will enhance the accuracy of tracking microscale targets in soft tissue.

DEDICATION

To my parents

Ahmad Talebian, Farzaneh Farahmandi

and

My beloved brother

Farzad Talebian

ACKNOWLEDGMENTS

I take this opportunity to thank my adviser Dr. Jit Muthuswamy for his guidance and support throughout my Masters work. His sincerity, patience and knowledge is truly admirable. I also would like to appreciate my committee members, Dr. Bruce Towe and Dr. Christopher Buneo for taking time evaluating my work.

I would like to extend my thanks to our PhD student, Swathy Sampath Kumar and research assistant professor, Dr. Arati Sridharan for helping me out in some of the experiments and brainstorming.

Last but not the least, I am truly indebted to my parents and brother for their love, support and guidance. Without their blessings, I would have not reached at this stage.

TABLE OF CONTENTS

	Page
LIST OF FIGURES	1
CHAPTER	
1 INTRODUCTION	4
Advantage of Moveable Microelectrodes	5
Tissue Response to Movable Microelectrodes.....	7
Tissue Micromotion	7
Variabilities in Neural Recording.....	9
Physical Changes-Variability in Neural Recording	9
Neuron Tracking Issue.....	10
Stability of Neural Recordings	11
Single- Unit Stability	11
2 LATERAL STRESS PROPAGATION DUE TO MICROELECTRODE.....	13
IMPLANTATION IN SOFT TISSUE.....	13
Objective	13
Mechanical Properties of Brain Tissue	13
Materials and Methods	18
Agarose Hydrogel as a Bench-top Models of Brain Tissue	18

	Page
Preparation of 0.5% Agarose Gel	21
Experimental Set-up for Stress Measurement.....	21
Experimental Protocol	25
Estimating Stress	26
Estimation of Viscoelastic Parameters	26
Representative Stress Measurement in Response to Microelectrode Movement	27
Results.....	28
3 SPATIO-TEMPORAL DISTRIBUTION OF STRAIN IN BRAIN TISSUE DUE TO MOVEMENT OF MICROELECTRODE	36
Objective – To quantitatively assess the spatio-temporal distribution of strain induced by the movement of microscale probes in soft viscoelastic tissue.....	36
PDMS as a Bench-top Model of Rodent Brain.....	36
Materials and Methods	38
Experimental Set-up to Measure Spatial Distribution of Strain	38
Experimental Protocol	40
Block Matching Algorithm.....	42
Tracking Single Particles	47

Results	47
Discussion.....	55
REFERENCES.....	56
APPENDIX	
A MATLAB CODES	59

LIST OF FIGURES

Figure	Page
1: Force measurement data from a rat.....	16
2 Neuron behaves as a moving target in viscoelastic tissue	17
3 Comparison between brain tissue and agarose gel	19
4 Force measurement data from the brain tissue of a rat	20
5: Force measurement data from agarose hydrogel	21
6: Experimental set up for force measurement	23
7: Software code to move microelectrode and measure forces.....	24
8: Schematic of experimental set up with two electrodes in agarose gel.....	25
9 Stress profile for 7 steps of downward movement at $x=0$	29
10: Averaged stress values for 30 μm downward movement, curve has been fitted to the data based on Prony series model	30
11: Force measurement result at $x=0$ for bidirectional movement of 60 μm downward followed by 30 μm upward.....	30
12 Consecutive stresses at a distance of $x=500 \mu\text{m}$ from a second microelectrode moving unidirectionally 30 μm steps downward with 3 minutes IMI.....	31
13: Averaged stress values for 30 μm unidirectional downward movement. A second order Prony series model shown in blue has been fit to the data	32

Figure	Page
14: Consecutive stress measurement for unidirectional 30 μ m downward movement with 3 minutes IMI ,at x=1000 μ m	33
15 Averaged stress values for 30 μ m downward movement. A Prony series model has been fit to the data for an inter-electrode distance of x=1000 μ m.....	33
16 Force result for bidirectional movement of 60 μ m downward followed by 30 μ m upward at x=1000 μ m	34
17: Average stress measurement for 30 μ m unidirectional downward movement at three different inter-electrode distances, x=0,x=500,x=1000 μ m.....	35
18: Average stress measurement for 30 μ m bidirectional downward movement at two different inter-electrode distances x=500,x=1000 μ m	35
19 : Force measurement data obtained from a rat.....	37
20 Force measurement data obtained from PDMS.....	37
21 Experimental set up for strain distribution measurement	39
22: A frame from initial movement of electrode inside the PDMS. Microscale beads are shown as white dots	41
23 A frame after the initial penetration of electrode inside the PDMS.	42
24 Motion vector for the initial penetration of electrode. Frames are one second apart. .	44
25: Motion vectors for the time microelectrode stopped movement, after 1mm penetration. Frames are one second apart.	45
26: Motion vector for the end of the relaxation time. Frames are two minutes apart.....	46

Figure	Page
27: Strain measurement for unidirectional movement of 30 μm downward with 3 minutes IMI. Three different particles at three different locations from the tip of the microelectrode were evaluated	48
28: Corresponding force measurement for unidirectional 30 μm downward movement.	49
29: Strain measurement for bidirectional movement of 60 μm downward with 1 minute IMI followed by 30 μm upward with 2minutes IMI. Three different particles at three different locations from the tip of the microelectrode were evaluated	50
30: Corresponding force measurement for bidirectional 60 μm downward movement with 1minute IMI followed by 30 μm upward movement with 2 minutes IMI.....	50
31: Strain measurement for bidirectional movement of 40 μm downward with 20 seconds IMI followed by 20 μm upward with 20 seconds IMI. Three different particles at three different locations from the tip of the microelectrode were evaluated	51
32: Corresponding force measurement for bidirectional 40 μm downward movement with 20 seconds IMI followed by 20 μm upward movement with 20 seconds IMI	52
33: Strain measurement for unidirectional movement of 20 μm downward with 40 seconds IMI. Three different particles at three different locations from the tip of the microelectrode were evaluated	53
34: Corresponding force measurement for unidirectional 20 μm downward movement with 40 seconds IMI.....	54

CHAPTER 1:

INTRODUCTION

Implantable microelectrodes are used to monitor neuronal activity in the brain in vivo. However, they have serious limitations both in acute and chronic experiments. As a potential solution to overcome the challenges with the fixed implantable microelectrode, movable microelectrodes has been suggested. Movable microelectrodes would maximize the quality of neuronal recording by adapting their position in the brain tissue. As an advantage of implantable microelectrode technology, is that it allows real time monitoring of single neurons while animal is behaving. They are a few common limitations of the microelectrode technology during the time of implantation or recording, such as biasing toward the active sample of neurons or the ones which have higher firing rate. They are a few factors involved in the yield of multi-channel electrodes that make it inconsistent during the experiments such as user skills, experimental set up and protocol and location of the electrode. Although monitoring single neuron or ensembles of neurons over a few weeks or months is of value to neuroscientists, with current implantable microelectrode technology, neural recording is unreliable in a long term experiments. (Vetter et al., 2004; Engel et al., 2005; Polikov et al., 2005). The mentioned drawback is of importance in some applications such as cortical prosthesis in which, single neuron or ensembles of neurons activity are being monitored.

Advantage of Moveable Microelectrodes

Movable electrode technology can re-establish contact at failed interfaces by repositioning the electrode (Jackson et.al, 2010). They are a few advantages with the technologies that allow us to move microelectrodes after implantation. These technologies will allow us to isolate single neurons activity and maintain neural recording for a longer duration. With these technologies, changes in small population of single neurons, such as for example, neuronal plasticity, can be monitored. Also, signal to noise ratio in the neural recordings can be enhanced. These technologies enable us to seek specific neurons after implantation, such as the ones that have been silent at the time of implantation. Movable microelectrodes can potentially be useful for applications which need neural recording for the life time of the patient. To record action potential of neuron, microelectrode have to be positioned within ten or hundreds of micron. However, this distance depends on type and orientation of the neuron. Therefore, if we are able to make small adjustments to the position of the microelectrode after implantation, microelectrode can be held in within the recording radius of a neuron. Single neuron recording over a long period of time with a fixed electrode is challenging specially in non-human primates. To confirm that recording has been done on a specific neuron over a long period of time (single neuron recording), a few methods can be used such as:

- 1: Clean inter spike interval (ISI),
- 2: Consistent shapes and peak to peak amplitude of signal and consistent behavioral correlates.

However, since different neurons can have identical action potential, the mentioned methods can not guarantee an identical neurons. In addition, action potential for the same neuron might change as a result of neuronal plasticity. Recording systems can monitor changes in signal amplitude, shapes and ISI. These systems will allow for the development of the predicative models to confirm the reason for recorded changes. As mentioned earlier, these changes might be because of neuronal plasticity or due to a change in the identity of a neuron (Tolias et al., 2007; Dickey et al., 2009). In contrast, in non-human primates, movable microelectrodes can achieve stable single neuron recording over a long time. (Yamamoto and Wilson, 2008 and Jackson and Fetz, 2007). It has been shown that the ability to reposition the microelectrode after implantation increases the yield and signal to noise ratio of the neuronal recordings. (Fee and Leonardo, 2001, Cham et al., 2005; Wolf et al., 2009). Neuron migration happens as a result of tissue reaction around the microelectrode or relative micromotion between the microelectrode and tissue. The mentioned biological reasons would result in loss of signal. Movable microelectrode gives us the ability to search for new neurons. Therefore, by using movable microelectrodes, the reliability of neuronal recording over a long time experiments as well as in clinical application such as cortical prosthesis will be increased. They are a few methods for movement of microelectrodes after implantation such as piezomotor (Yang et al., 2011), step-per motors (Fee and Leonardo, 2001; Kern et.,al,2008), hydraulic positioning (Decharms et al., 1999; Sato et al.,2007). These technologies have been tested in mice, rats, song birds and non-human primates. All of the mentioned technologies were successful in different levels. They are a few issues with manual movement of microelectrodes such as

constraining the animal during the movement of microelectrode. This may affect its spontaneous behaviors such as motor activity. The other possibility is resisting of the animal and perturbing the position of the microelectrode. Therefore, motorized microelectrodes are more reliable compared to the manual one. Movable microelectrodes will result in enhanced signal quality (Jackson and Fetz, 2007; Yammoto and Wilson, 2008; Wolf et al., 2009; Jackson et al., 2010). Movable microelectrodes can isolate single units and result in stability of recordings for weeks (Fee and Lenardo, 2001). They will also result in improved yield as well as simultaneous monitoring of pairs. There are a couple of key gaps in understanding of neuron-electrode interface that will affect the quality of neuronal recording are 1) response of the brain tissue surrounding the microelectrode and 2) relative micromotion between electrode and brain tissue.

Tissue Response to Movable Microelectrodes

In acute experiments, implanted microelectrodes cause inflammatory and body response (Szarwski et al., 2003; Polikovet al., 2005 ; Stice and Muthuswamy, 2009). According to these studies glial sheath formation around the microelectrode has happened after 4-6 weeks of implantation. Neural migration away from the microelectrode has been also seen.

Tissue Micromotion

Another issue is the relative micromotion between the microelectrodes which is fixed to the skull and the surrounding brain tissue. There are a few reasons that cause brain tissue to move relative to the microelectrodes such as pulsation in the vasculature and propagating

mechanical pressure waves due to breathing and due to animal behavior (vigorous movement of the head, sneezing etc). The level of tissue micromotion depends on species. Cats and humans have the larger relative displacement compared to rodents. Due to vascular pulsation, displacement of 100-250 μm and due to breathing, displacement of 300-900 μm were observed in cats (Britt and Rossi, 1982). It has been observed that anesthetized rat models have tissue displacement of 1-4 μm due to pulsation in the brain vasculature. In humans, brains can displace over several millimeters from accelerated head movement. Neuroscientists are interested to know the impact of the relative displacement between the recording microelectrode and brain tissue on recordings from a single neurons in the brain. Is the Movable microelectrode technology the solution for the issue of tissue micromotion? Unfortunately, according to the data on micromotion between implanted electrode and surrounded brain tissue, there is no solid answer for this question. However, short term studies demonstrated that tissue micromotion have an important impact on the electrical recordings from single neurons. This impact is twofold, which means there is a direct (short-term) and indirect (long-term) impact. There are several results to show the short term impact of micromotion. These results show change in electrical recording from single neurons (Chestek et al., 2009). Several studies show that manual or motorized movement of microelectrodes results in restoration of fading neuronal signal and results in enhanced neuronal recording (Jackson and Fetz, 2007). Studies show that loss or deterioration of recording from a specific neuron will happen by an increase in distance between the microelectrode and the recorded single neuron. Neuroscientist are interested to know how a behavioral movement of the animal may lead to changes the electrical

recording. Intuitively, relative displacement between the recording site of the microelectrode and the neurons in the surrounding brain tissue will lead to changes in amplitude and shape of the recorded action potential. Since brain tissue is viscoelastic, it is complicated to be able to predict any changes in the electrical recording from a single unit due to relative micromotion between the brain tissue and the recording microelectrode. Therefore, the real distance between the microelectrode and neuron is different compared to the propagating pressure waves which happens mainly due to animal behavior.

Variabilities in Neural Recording

There are several reasons for variation in neural signal recording such as motion artifacts, brain micromotion and presence of glial sheath due to the immune response of the tissue to the implanted electrode. However, tissue response is the main factor for instability in neural recordings. Electrode insertion and movement damages the extracellular matrix, glial and neuronal cell processes. Tissue in the region of electrode track is pushed aside and tissue under the electrode tip is compressed. As a result, high stress region around the electrode will be built.

Physical Changes-Variability in Neural Recording

Physical changes at neural interface is one of the source of variation in neural activity. During electrode penetration, tissue strains as the tissue is pulled with the electrode. Physical changes happens when the microelectrode and tissue move relative to each other. Mechanical properties of material will determine how it returns to a steady state. Tissue

displacement causes change in relative position between the neuron and the recording site of the microelectrode.

Neuron Tracking Issue

A common issue during extracellular neural recording is that a single electrode's signal may have spikes which are generated by other neurons near the electrode tip. The ultimate goal of extracellular recording is to detect the activity of individual neurons. Therefore, each detected action potential must be associated to the neuron that produced it, which is called spike sorting. Shape of spikes are very similar across neurons and spike sorting algorithms classify action potential according to waveform shape and amplitude. Accurate spike sorting is important in electrode positioning. The goal here is to maximize signal quality. Spike sorting, due to its importance, is a task that is typically achieved through a largely manual process in experiments, through visual examination of spike waveforms. It should be noted that, if spikes are incorrectly classified, the metrics from the signals of each distinct neuron would be corrupted. In the autonomous electrode positioning algorithm spike sorting is achieved in an unsupervised manner. Since electrode signal is sampled over many brief and successive recording intervals, it is important to note that spikes should be associated to their generating neuron within specific recording interval. Besides, signals from the same generating neuron must be associated with each other across recording intervals. Therefore, it is important for the algorithm to be able to track individual neurons over successive intervals to evaluate whether a change in electrode position has

improved the signal quality of these neurons. That said, two data association challenges must be addressed:

- 1) Classification or clustering which is the process of grouping action potentials from a single interval into the distinct sets.
- 2) Tracking is the process of associating clusters to each other across recording intervals and determining whether they are from the same group or not.

In multi-unit recordings in electrophysiological experiments, automating the spike sorting task can remove the extensive task of manual sorting from experimenters and improve the accuracy of the result. It has been reported that manual sorting is inconsistent.

Stability of Neural Recordings

Data for stability analysis is recorded from:

- 1) Day to day recording sessions which last maximum of few hours
- 2) Continuous recording session over 24 hours
- 3) Long term recordings (chronic recordings) over several months.

Single- Unit Stability

Since intra-cortical microelectrode array has the ability to simultaneously record from large populations of neurons over long period of time, the use of these arrays has been extensively common in neuroscience experiments. Unfortunately, it is not clear that neuronal signals achieved in multiple recording sessions come from the same neuron or not. Many methods has been reported to assess single unit stability such as measuring the similarity of 1) average spike waveform and 2) inter-spike interval histogram. The goal of

identifying stable neurons is to study long term learning effects across days as well as for the development of brain-machine interfaces. A few groups have reported stability data by using a method which is based on the similarity of spike waveform shapes. It has been reported that tracking a neuron is practical by visual inspection over a few weeks, however, they did not quantify the results. In many studies, such as Jackson and Fetz (2007) they do not include an estimate of false positive rate which is the probability that signals from two different neurons would be classified as stable. A common mistake is that stable units are assumed to have similar waveforms, however, different neurons can also have similar waveforms.

Another issue is that recordings from one channel usually contain activity from more than one neuron. Although a movable electrode can be positioned in a way that isolates single units, it is not possible with a chronically implanted microelectrode array. Therefore, there are two ways to track neuronal stability on these arrays.

- 1) Only the channels with almost no contamination from noise or other neuronal signals should be used. This means potentially meaningful data would be discarded
- 2) Do the spike sorting on the neuronal signals to reduce this contamination.

CHAPTER 2

LATERAL STRESS PROPAGATION DUE TO MICROELECTRODE IMPLANTATION IN SOFT TISSUE

Objective

In this chapter, we are discussing lateral stress propagation during microscale navigation inside the brain tissue. As mentioned earlier, step movement of microelectrode inside the brain tissue induces stress in the surrounding brain tissue. In this study, the effect of lateral stress due to the movement of one electrode on the other electrode has been evaluated.

Mechanical Properties of Brain Tissue

As mentioned earlier, brain tissue is viscoelastic. The best model for brain tissue is the one which is considered as hyperelastic and viscoelastic medium (Miller et al. 2000). As an example of constitutive model is viscoelasticity. Viscoelasticity model has been used for the materials which has the time dependent property to a stress or strain. A main property of viscoelastic materials is dissipation of energy under loading condition. This phenomenon has been known as hysteresis. This indicates that in strain-stress curve, loading portion is higher compared to unloading portion. However, this phenomenon has not been for purely elastic material. This implies that the relationship between stress and strain for a spring is linear , which means that loading portion and unloading portion are

the same. When electrode is moving forward in the brain tissue, it is considered as loading portion. Backward movement of the electrode is considered as unloading portion.

Experimental results showed the nonlinearity of stress and strain in brain tissue (Miller 2000). Since a linear viscoelastic model cannot fully describe the material characteristics of brain tissue, a hyperelastic viscoelastic model is used.

Hyperelasticity is used as a type of constitutive model to explain nonlinearity between stress and strain in brain tissue.

Viscoelastic materials are known for two main characteristics: creep and relaxation. In creep, viscoelastic material, under constant stress, would undergo deformation. This deformation would continue until asymptotic level of strain is reached. In relaxation, stress level in brain tissue reaches its maximum and it relaxes over time. Response of the brain to the step perturbation of stress or strain should be determined by these two characteristics.

There are two main assumptions for the model of brain tissue:

- 1) Since there are microvasculature and tissue heterogeneity inside the brain tissue, microscale movement of electrode inside the brain tissue would be consider as anisotropic. However, it has been assumed that the properties of brain tissue are isotropic. This means that mechanical properties of brain tissue are the same in all directions.
- 2) When electrode moves inside the brain tissue, tissue would be displaced along the electrode track. This causes deformation around the electrode. However, it has been assumed that brain tissue is incompressible.

Viscoelastic and hyperelastic properties of brain tissue have made the prediction of any change in the electrical recording from the single neuron complicated. As mentioned earlier, this change in electrical recording happens because of the micromotion between the brain tissue and recording microelectrode. Movement of the electrode makes a trend as a function of time between the real distance of the recorded neuron and recording site of the electrode. Therefore, a step movement of the electrode can be modeled as an induced strain. Forward movement of the electrode causes compression of the brain tissue. The forward movement causes stress in the surrounding brain tissue. The induced stress level due to the movement of microelectrode, reaches a maximum value and then relaxes over time. Backward movement of the electrode causes tensile stress. The relaxation time constant R is the time it takes the stress level reaches one-third of the initial value under constant strain. It shows the time taken for the compressed tissue to relax to the steady state level. Thus, one step movement of the electrode causes the real distance between the electrode and the neuron to evolve as a function of time. Steady state will achieve at least after a $4 R$ time interval.

This is of importance for mapping SNR as a function of electrode position in brain tissue. The goal is to find an optimal site for which SNR is above the defined threshold. If the relaxation time constants are not included in the model, the relative distance between the electrode and a neuron would change with time. This indicates, SNR changes with time. Thus, after the relaxation of the tissue, electrode needs to be repositioned to adjust for new SNR. This issue continues in a cycle and neuron would become a moving target. Although the exact viscoelastic constant of brain tissue under small levels of strain is unknown, strain

values should be the input in to the mechanical model of the brain tissue to be able to find the relaxation time constant. Then, stress response and the time taken to reach steady state will be calculated.

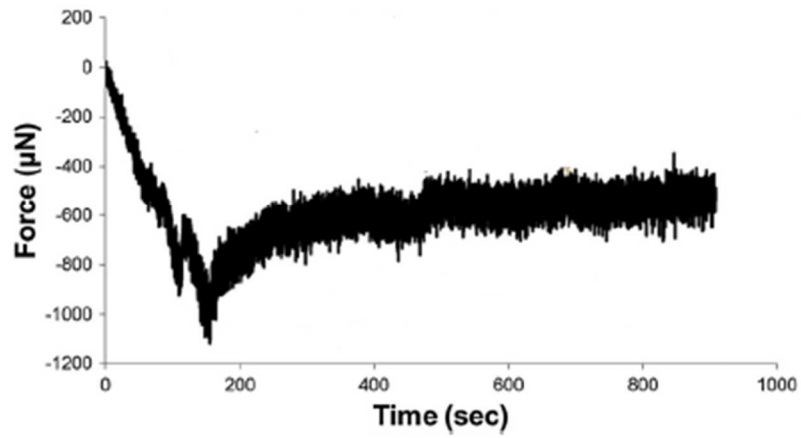


Figure 1: Force measurement data from a tat

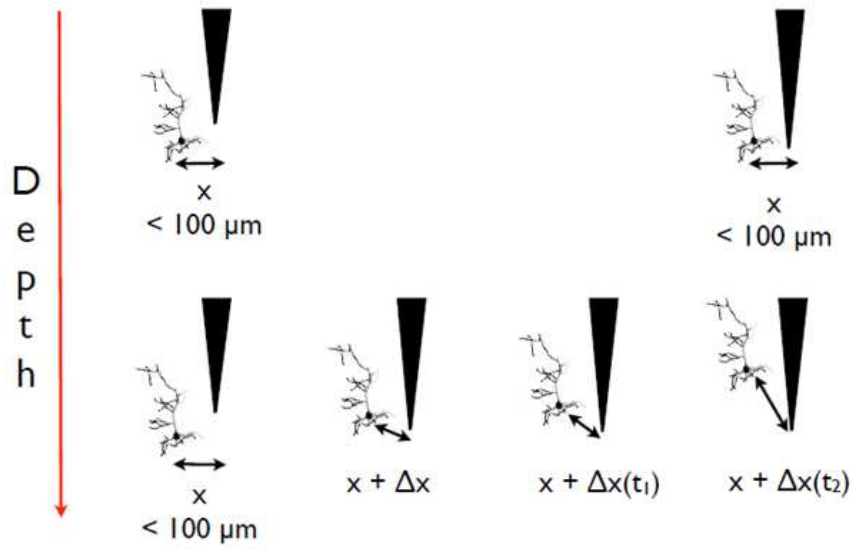


Figure 2 Neuron behaves as a moving target in viscoelastic tissue

Materials and Methods

The goal of this research was to study the effect of forces from microelectrode- tissue interaction in a simple, inexpensive, and robust model system to be used as an in vitro surrogate for in vivo brain tissues. Forces from microelectrode- tissue interaction during microscale navigation in an agarose gel were measured. From these force measurement, stresses on the surrounding brain tissue were calculated.

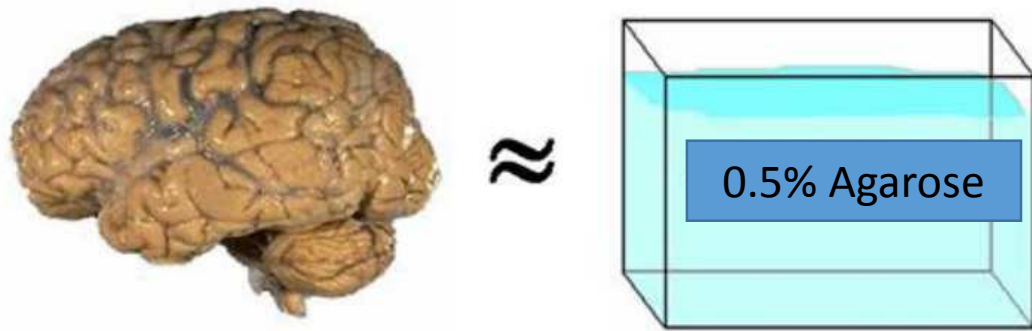
Agarose Hydrogel as a Bench-top Models of Brain Tissue

For in vitro studies, agarose gel was chosen to serve as a model of brain tissue.

Justifications for this choice of material are summarized in Fig 3. First, both brain tissue and agarose gel can be considered poroelastic materials. Although overall the brain is inhomogeneous and anisotropic in its composition, localized regions of gray matter can be largely homogeneous and isotropic, like agarose gel.

Agarose gels have been used to evaluate the dynamic response of soft tissues. In dynamic experiments studying the brain response to impact loading, gel materials are used. Gels are simpler in handling and can be made in large quantities. In such experiments, it is clear that the dynamic mechanical behavior of the gels must be similar to that of the brain tissues they are representing. The behaviors of the agarose gel are then compared to that of the brain tissues under identical loading conditions to find candidate gel materials that respond to dynamic loading in a similar manner as the brain tissues. The results show that

the mechanical properties of agarose gel with concentration of 0.5% are close to that of brain tissues.



Property	Brain	Agarose Gel
Material Type	Poroelastic	Poroelastic
Homogeneity	Inhomogeneous	Homogeneous
Isotropy	Anisotropic	Isotropic
Optical Properties	Opaque	Transparent
General Properties	Vary among brains	Highly reproducible
Availability	Limited supply	Unlimited supply

Figure 3 Comparison between brain tissue and agarose gel

Figure 4 shows the force-displacement curve from rat's brain tissue. Figure 5 shows force-displacement curve from agarose gel. In both cases, electrode was moved 1 mm inside and it was left in place until forces reached steady state. As shown in Fig. 4, maximum force on the brain tissue is 1000 μN and it is comparable with maximum

force exerted on agarose gel after 1mm penetration. Therefore, we decided to do this study in agarose hydrogel as it is a simple model of brain tissue.

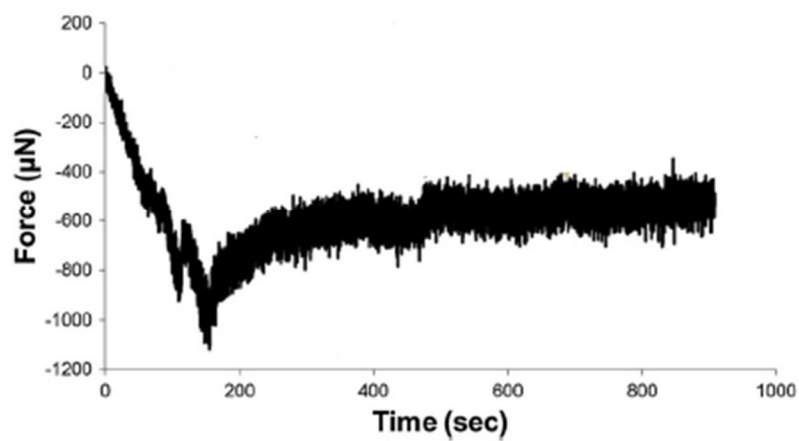


Figure 4 Force measurement data from the brain tissue of a rat

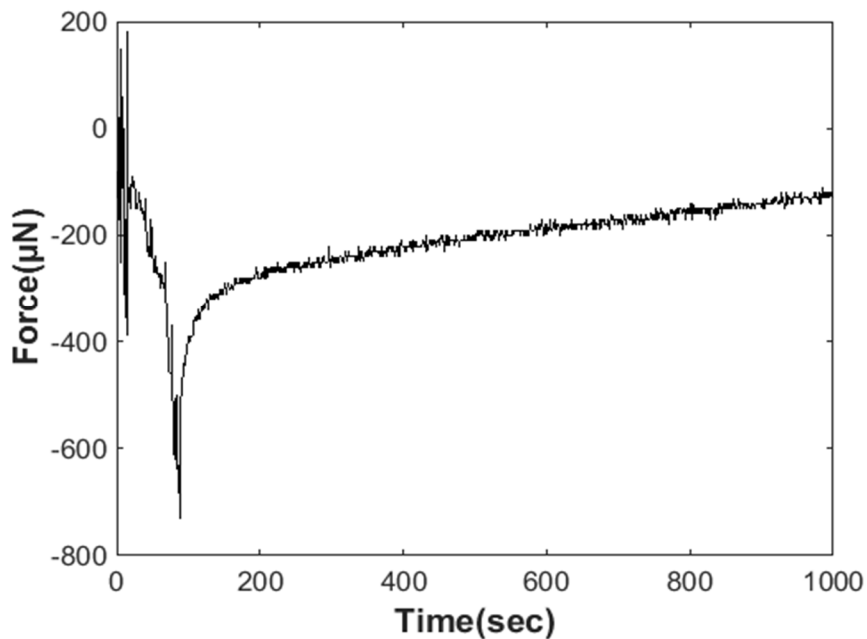


Figure 5: Force measurement data from agarose hydrogel

Preparation of 0.5% Agarose Gel

Bench-top model of brain tissue, 0.5% agarose hydrogel, were prepared by mixing 0.5 grams of dry agarose (X) with 100 mL sodium chloride. Then the solution was warmed up to a boiling point for 10 min. Solution was poured into the gel dish.

The gel was allowed to cool down and solidify for 30 minutes.

Experimental Set-up for Stress Measurement

In this study, AM systems (Carlsberg, WA) tungsten microelectrodes were used. Microelectrode had a 127 µm shaft diameter with 8° taper and 76.2 length. In figure (), experimental set up is shown. A single microelectrode was attached to a hydraulic

micromanipulator (FHC# 50-20-1C, Bowdoin, ME). and the second microelectrode was attached to a precision 10 g load cell (Futek, LSB210, Irvine, CA) and then mounted on the manual micromanipulator. Increase in force readings was an indication of contact with the surface of the agarose gel. These two electrode electrode and manually lowered in the gel and implanted to a depth of 1mm below the gel. Once implanted, it was left in place for about 30 minutes. During this time, forces would settle to steady state and the gel around the microelectrode would stabilize. After that, the second microelectrode was also lowered in the gel at the rate of 100 $\mu\text{m/s}$ and implanted to a depth of 1 mm below the gel. Once implanted, second microelectrode was also left in place for about 30 minutes to allow forces to settle to steady state. The microelectrode was moved according to pre-defined movement patterns in each experiments and resulting forces was recorded. In order to move the microelectrode in specific step size with precise interval between steps and control the direction of the movement, the movements of the electrode were automated. A hardware hack on the FHC hydraulic manipulator that was manually controlled was performed by interfacing the remote control pin in the front panel with the TTL ports of a computer that generates voltage pulses according to a programmed movement pattern. A LabView based platform generates TTL pulses that control the step size, IMI and the direction of movement of the microelectrode.

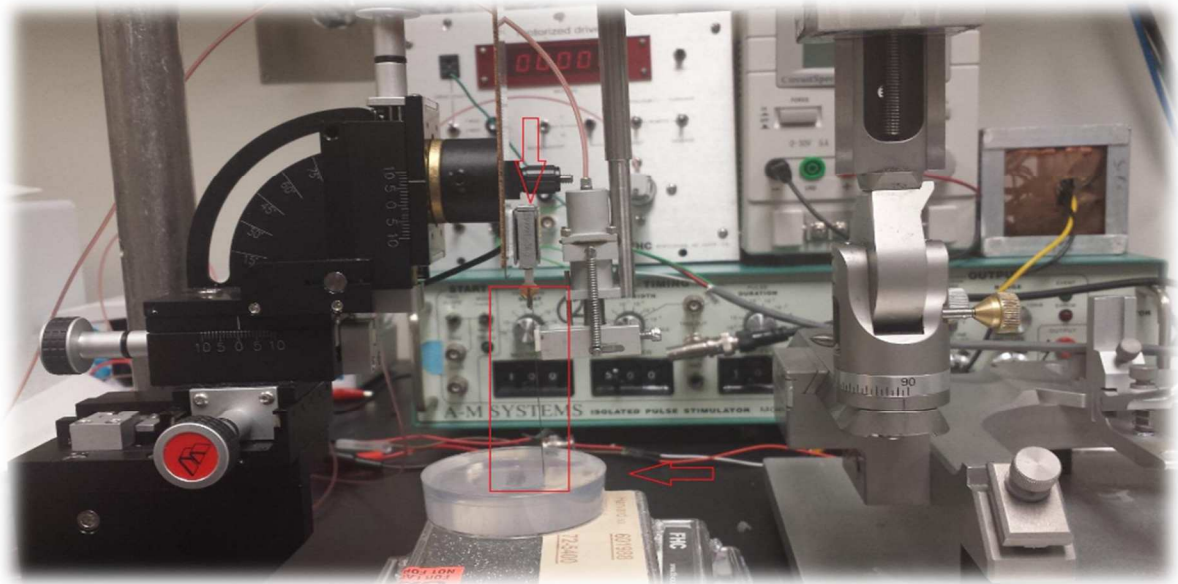


Figure 6: Experimental set up for force measurement

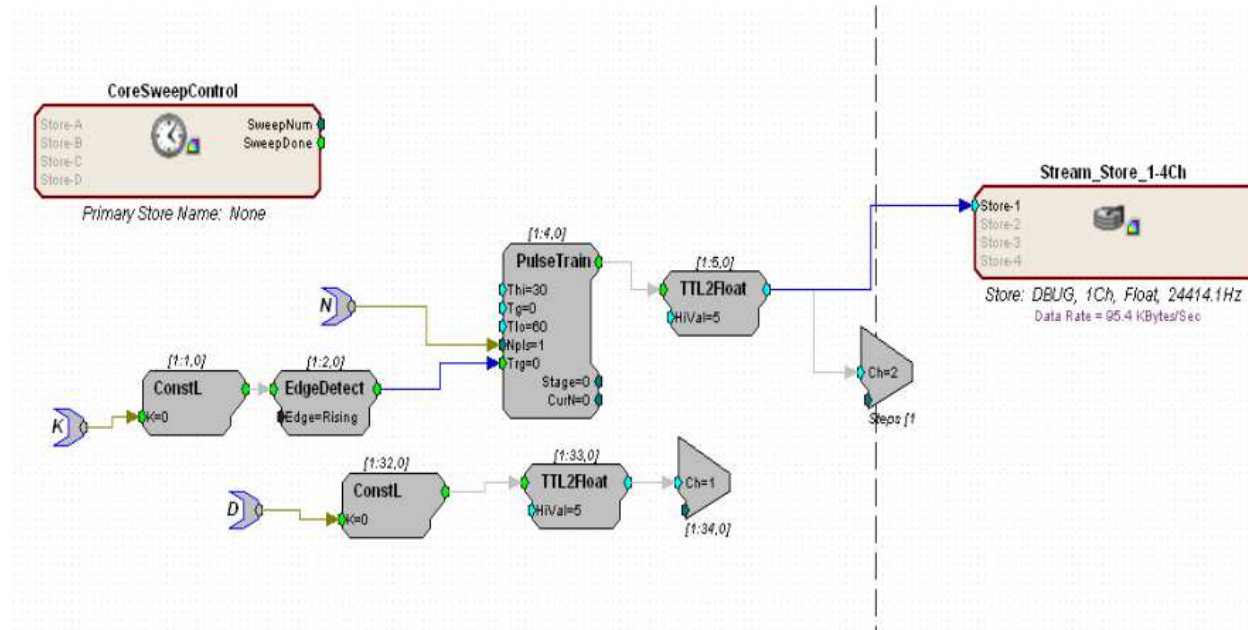






Figure 7: Software code to move microelectrode and measure forces.

Experimental Protocol

In this study, four different movement patterns were studied. 1: Unidirectional movement of 30 μm and 3 minutes inter movement interval (IMI). 2: Bidirectional, inchworm type movement of 60 μm and 1 minutes IMI followed by 30 μm downward movement and 2 minutes IMI. 3: Unidirectional movement of 60 μm movement and 20 seconds IMI followed by 40 μm upward movement and 2 seconds IMI.

As mentioned earlier, two electrode were placed next to each other with a predefined distances of 500 and 1000 μm . Each of four movement pattern was tested in all of the above inter-electrode distances. The rationale for choosing these distances between two electrodes is that we are looking for lateral stress propagation and we would like to study several distances under which stress propagation from movement of one electrode affect neural recording on the other electrode. A schematic of the placement of the microelectrodes is shown in Fig. 8.

- Load Cell 
- An Electrode 
- The Electrode which is creating the stress 
- Dish of Agarose Gel 
- X=Inter electrode distance

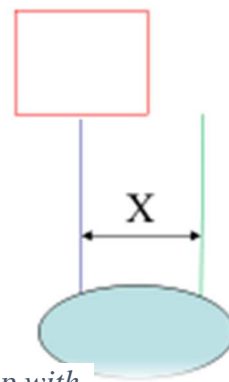


Figure 8: Schematic of experimental set up with two electrodes in agarose gel

Estimating Stress

The load cell records the forces acting on the microelectrode during microscale movement inside the brain tissue and during tissue relaxation. The stresses on the microelectrode are calculated as force per contact area. At each time point in the force curve, the surface area of the microelectrode while it is in contact with agarose gel is calculated.

According to the following formula, the measured force was divided by the contact area to get the total stress on the microelectrode.

$$\sigma = F/A$$

Estimation of Viscoelastic Parameters

Maxwell model is a well-known model in estimating the stress relaxation behavior of viscoelastic materials. $G(t)$ is the relaxation function and it is defined in terms of Prony series parameters. The stress relaxation response can be described by a viscoelastic model with a 2nd order Prony series expansion.

$$G(t) = G_1 e^{-t/\tau_1} + G_2 e^{-t/\tau_2}$$

In the above equation, $G(t)$ is the relaxation response as a function of time. $G(0)$ is the instantaneous shear modulus. It has been defined as maximum peak stress value measured when microelectrode is moved. Instantaneous shear modulus is an indicator of the stiffness of the brain tissue. Higher the modulus, stiffer the tissue. G_1 is the short term shear moduli

and G_2 is the long term shear moduli. These two parameters characterize the relaxation response of the brain tissue.

τ_1 and τ_2 short term and long term relaxation time constants.

Representative Stress Measurement in Response to Microelectrode Movement

As mentioned earlier, in this study, we are interested to find out the lateral stress propagation as one electrode is moving inside the soft tissue. Four different movement patterns has been executed.

- 1) Unidirectional downward movement of the electrode with 30 μm step size and 3 minutes inter movement interval (IMI).
- 2) Bidirectional downward movement of 60 μm step size and 1 minute IMI followed by 30 μm step size and 2 minutes IMI.
- 3) Unidirectional movement of the electrode with 20 μm step size and 40 seconds IMI
- 4) Bidirectional movement of 60 μm step size and 20 seconds IMI followed by 40 μm upward and 20 seconds IMI.

For each pattern, two different distances between two electrodes has been examined, 500 μm and 1000 μm . The forces measured are converted to stress values. Data recorded is smoothed using 32 point-averaging window. The characteristic stress for a unidirectional downward movement of a microelectrode, 500 μm away from the second microelectrode with 30 μm step size and 3 minutes IMI is shown in figure 9.

Time needed to achieve steady state forces varies with step size, the rate of movement and residual stresses due to the prior movement in the surrounding tissue. This is called hysteresis and it happens because of the time dependent mechanics of brain tissue.

During downward movement , forces inducing on the microelectrode represent both shear and compressive forces. Upward movement of the electrode register tensile forces on the load cell. These forces register positive increments in the registered force in the load cell.

Downward movement of the electrode causes compressive forces. Compressive forces register negative force increment in the load cell.

Results

Figure9 shows the stress propagation in agarose gel when the electrode which is creating the stress is $x=0 \mu\text{m}$ away from the second electrode. This means we only used one electrode with a load cell on it. The electrode was moved downward in 7 steps of $30 \mu\text{m}$ each with 3 minutes IMI.

The short term and long term relaxation parameters of the non-linear viscoelastic model were also estimated. All stress curve in Figure 10 were overlaid on top of the first curve and we took the average of them. Then the model fitting was done in MATLAB. The instantaneous shear modulus was calculated as the magnitude of the step change in stress value at each instant of movement. The same analysis procedures were performed for other movement patterns. Figure 11 shows stress due to bidirectional movement pattern for the

same experiment. As expected, stress value reached steady state after a few movement. As figure 11 indicates, stress value for $x=0$ is approximately 800 Pa.

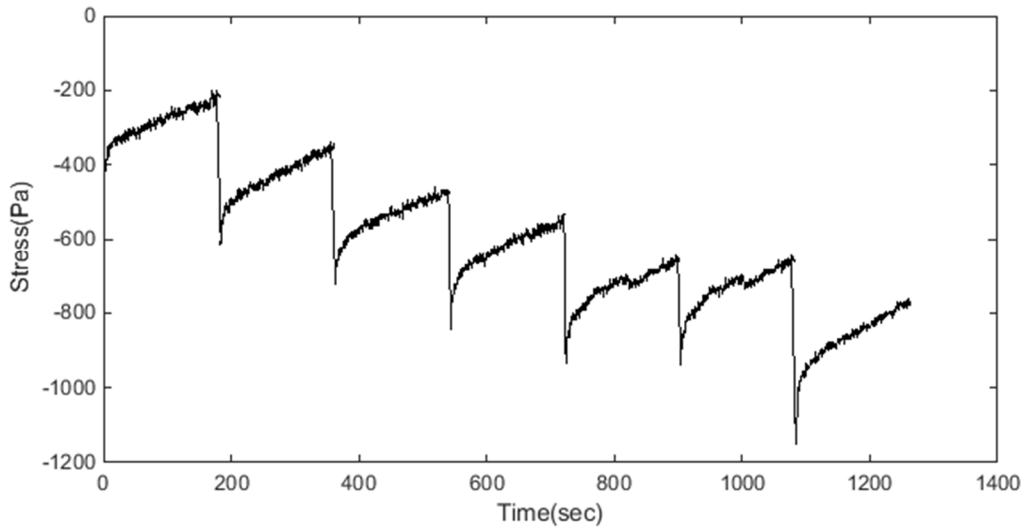


Figure 9 Stress profile for 7 steps of downward movement at $x=0$

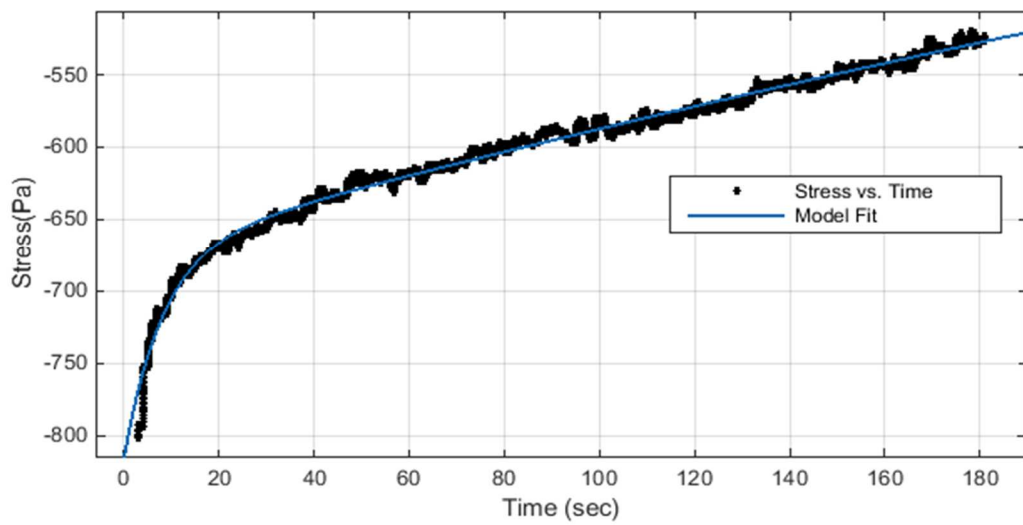


Figure 10: Averaged stress values for 30 μm downward movement, curve has been fitted to the data based on Prony series model

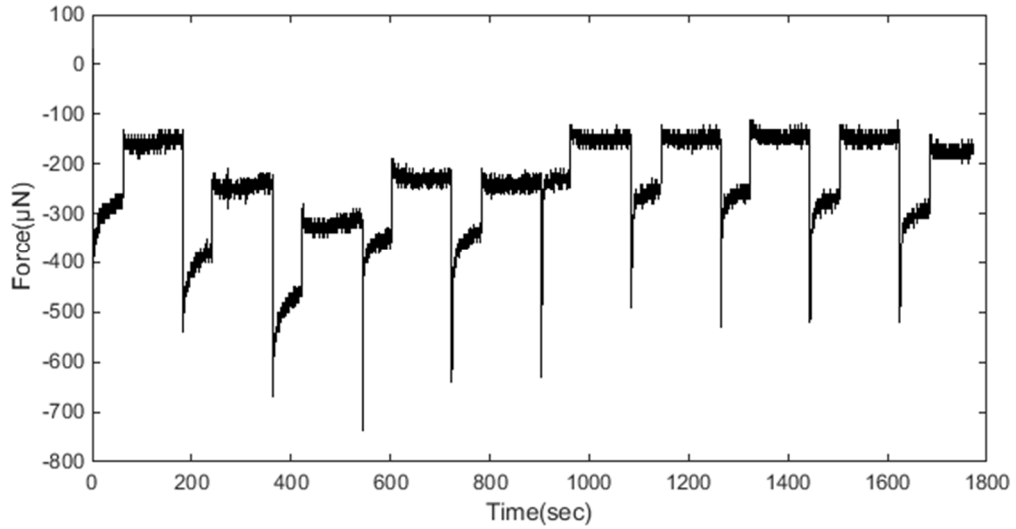


Figure 11: Force measurement result at $x=0$ for bidirectional movement of 60 μm downward followed by 30 μm upward

Figure 12, shows stress values as a result of 7 consecutive unidirectional movement of 30 μm with 3 minutes IMI for $x=500$. In this experiment, the electrode which is creating the stress is 500 away from the stationary electrode. Figure 13 shows the result of model fit. As it is shown in figure 13, stress values for $x=500$ μm is approximately 200 Pa.

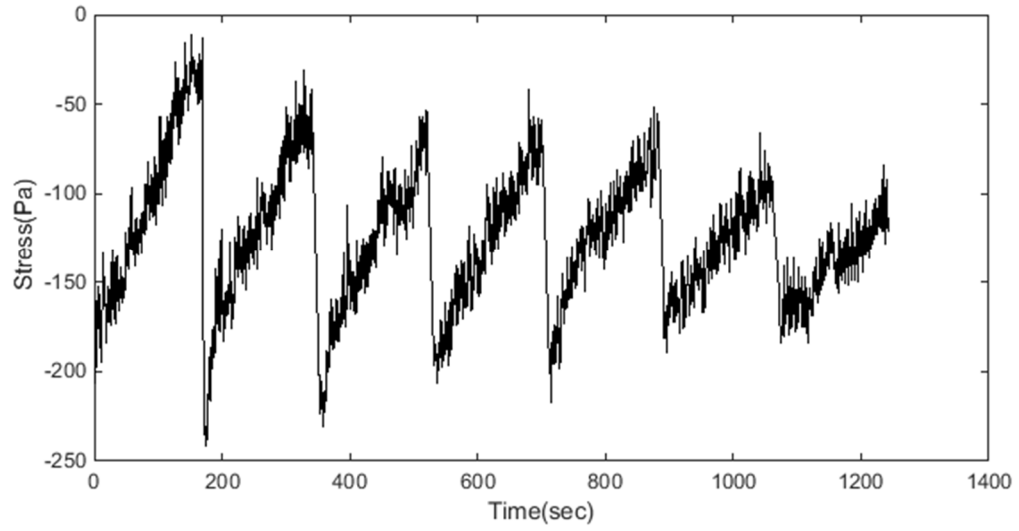


Figure 12 Consecutive stresses at a distance of $x=500\ \mu\text{m}$ from a second microelectrode moving unidirectionally $30\ \mu\text{m}$ steps downward with 3 minutes IMI

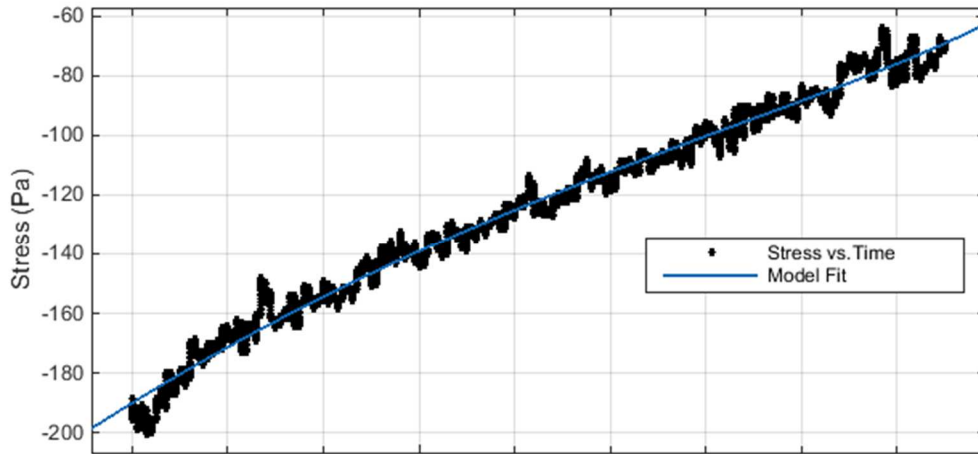


Figure 13: Averaged stress values for 30 μm unidirectional downward movement. A second order Prony series model shown in blue has been fit to the data

Figure14 shows stress due to 6 consecutive downward movement of 30 μm with 3 minutes IMI. In this experiment, $x=1000 \mu\text{m}$, meaning that the electrode creating the stress is 1000 μm away from the stationary electrode which is measuring the stress. Stress registered on the load cell is -120 Pa and is less compared to the corresponding values for $x=0$ and $x=500 \mu\text{m}$ distances .

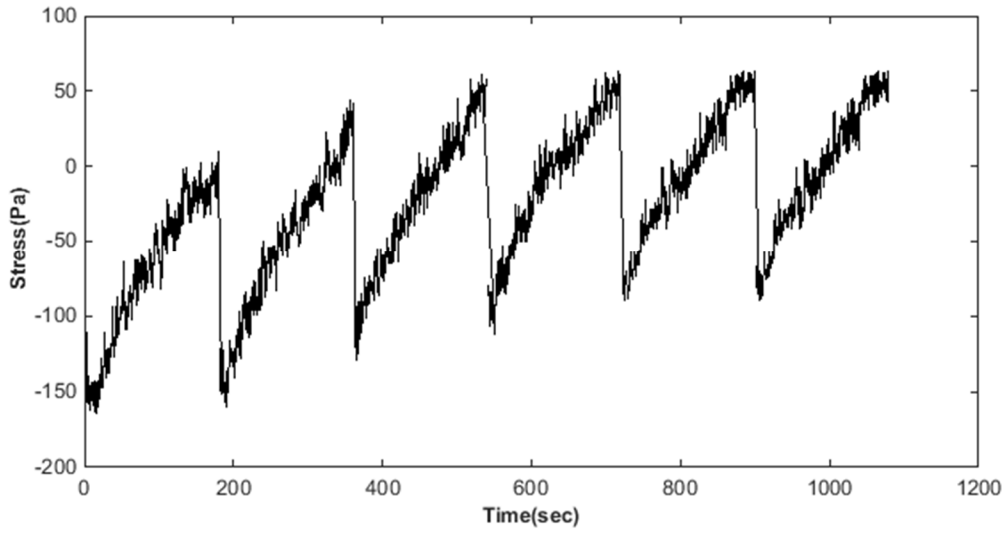


Figure 14: Consecutive stress measurement for unidirectional $30\mu\text{m}$ downward movement with 3 minutes IMI ,at $x=1000\mu\text{m}$

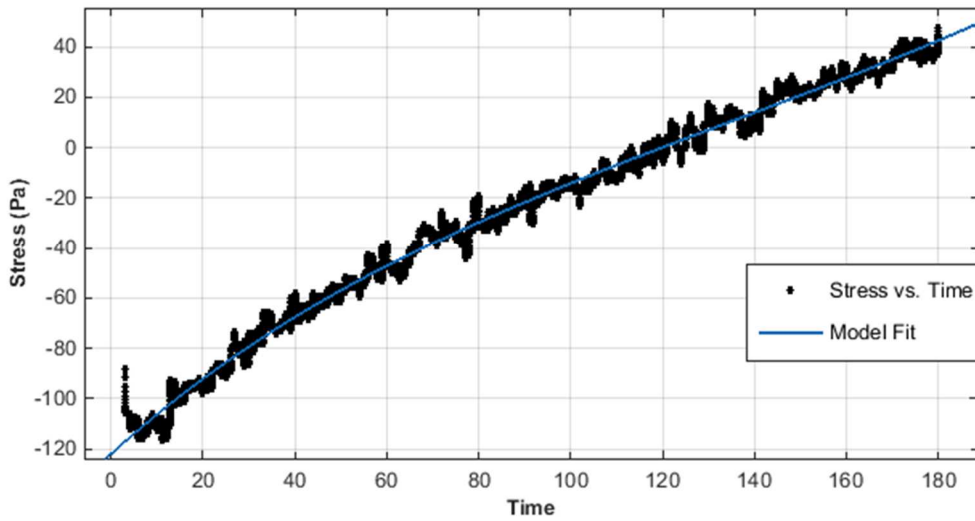


Figure 15 Averaged stress values for $30\mu\text{m}$ downward movement. A Prony series model has been fit to the data for an inter-electrode distance of $x=1000\mu\text{m}$

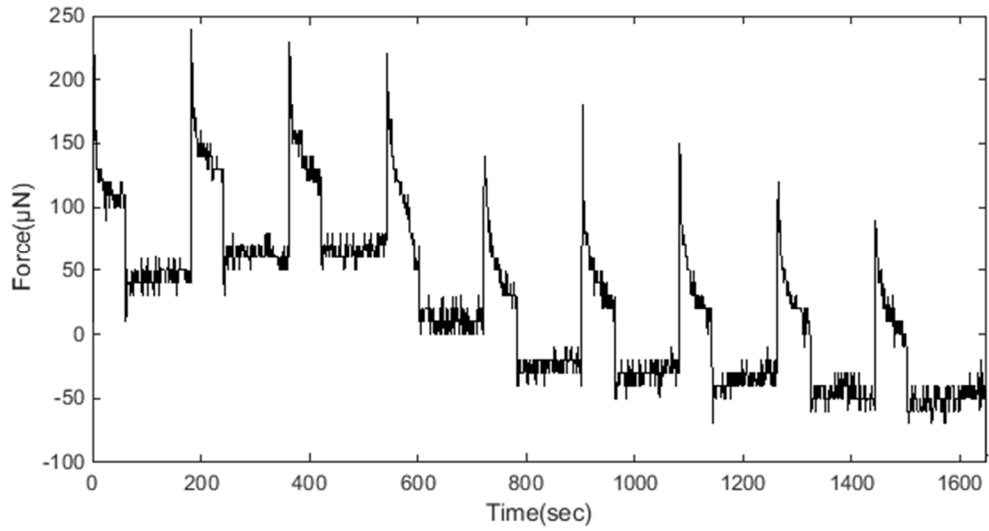


Figure 16 Force result for bidirectional movement of 60 μm downward followed by 30 μm upward at $x=1000 \mu\text{m}$

Figure 17 shows the result of stress measured for 3 different inter-electrode distances. As expected minimum lateral stress was measured when inter-electrode distance $x=1000 \mu\text{m}$.

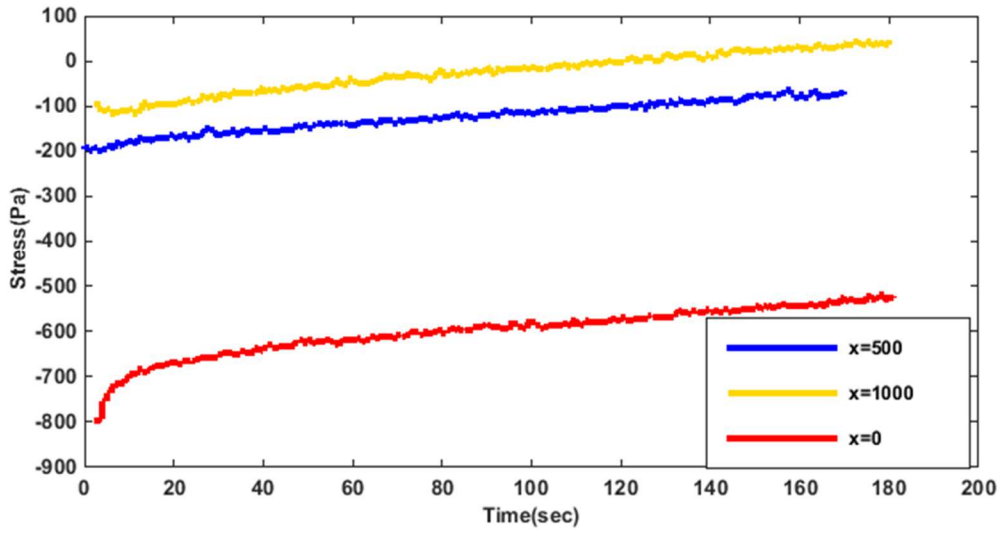


Figure 17: Average stress measurement for $30\ \mu\text{m}$ unidirectional downward movement at three different inter-electrode distances, $x=0, x=500, x=1000\ \mu\text{m}$

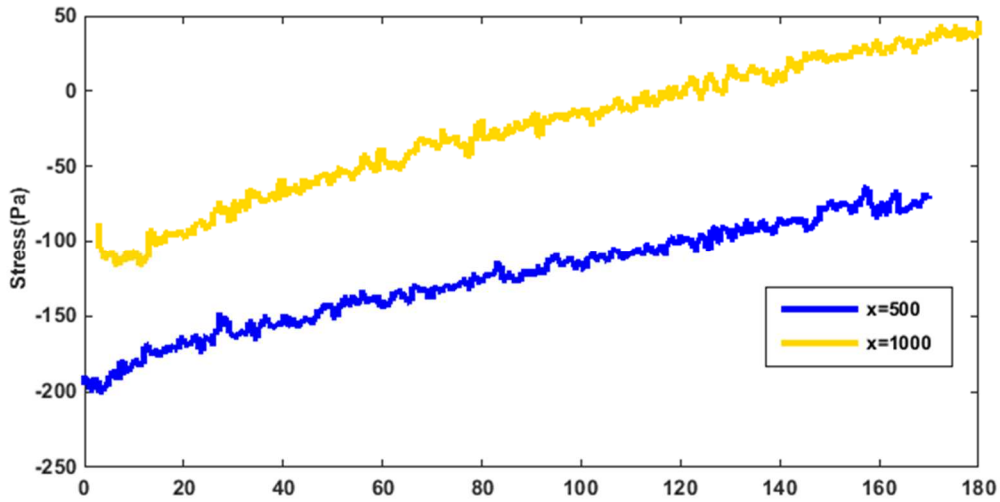


Figure 18: Average stress measurement for $30\ \mu\text{m}$ bidirectional downward movement at two different inter-electrode distances $x=500, x=1000\ \mu\text{m}$

CHAPTER 3

SPATIO-TEMPORAL DISTRIBUTION OF STRAIN IN BRAIN TISSUE DUE TO MOVEMENT OF MICROELECTRODE

Objective – To quantitatively assess the spatio-temporal distribution of strain induced by the movement of microscale probes in soft viscoelastic tissue.

PDMS as a Bench-top Model of Rodent Brain

To study the distribution of strain in space induced by the movement of microelectrode in soft tissue, we used another bench-top model of brain tissue, called PDMS. Due to solubility issues, we could not continue our study with agarose gel. Figures 19 and 20 show the force-displacement curves due to microelectrode movement in PDMS and brain tissue of the rat, respectively. As the figures indicate, maximum forces and dynamics of relaxation in PDMS are comparable with those measured in brain tissue indicating PDMS as a suitable bench-top model of brain tissue.

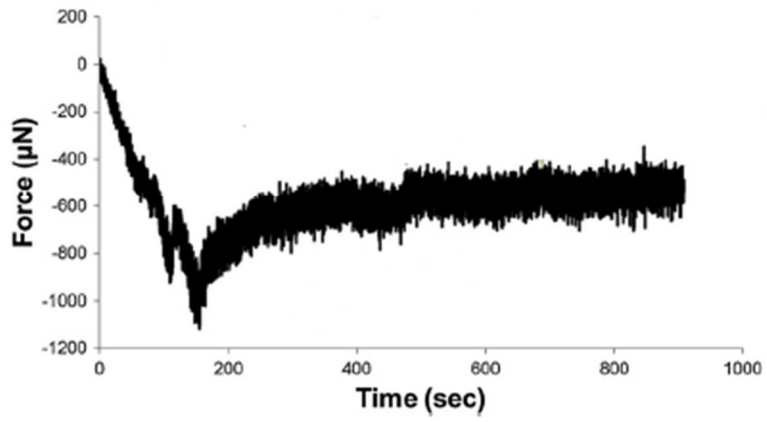


Figure 19 : Force measurement data obtained from a rat

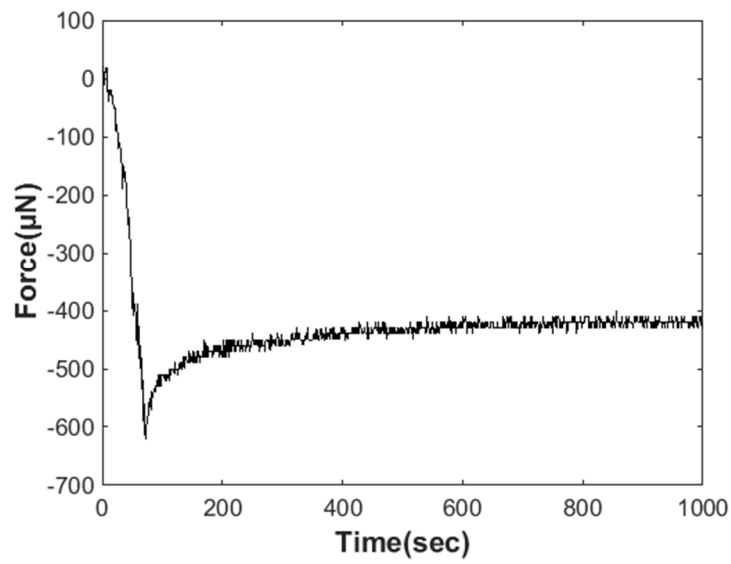


Figure 20 Force measurement data obtained from PDMS

Materials and Methods

In this study, Microspheres (Cospheric LLC) of diameter 10-27 μm were embedded in PDMS. As mentioned earlier, PDMS is a brain like material. Diameter of a neuron is between 10-20 μm , thus, we chose microsphere whose diameter is in the same range to be able to simulate neurons.

Experimental Set-up to Measure Spatial Distribution of Strain

For this section of the experiment, we were interested to quantitatively map the strain fields using video microscopy.

To do so, we used solution of microscale beads in PDMS dish. Imaging was done by placing the microscope in front of PDMS dish and connecting it to the computer. wmv format video was acquired with 29 frames/second. The video was converted to the frame by frame images. Based on the acquired data, we decided to compare frames every 30 seconds. Figure 21 shows experimental set up for strain measurement.

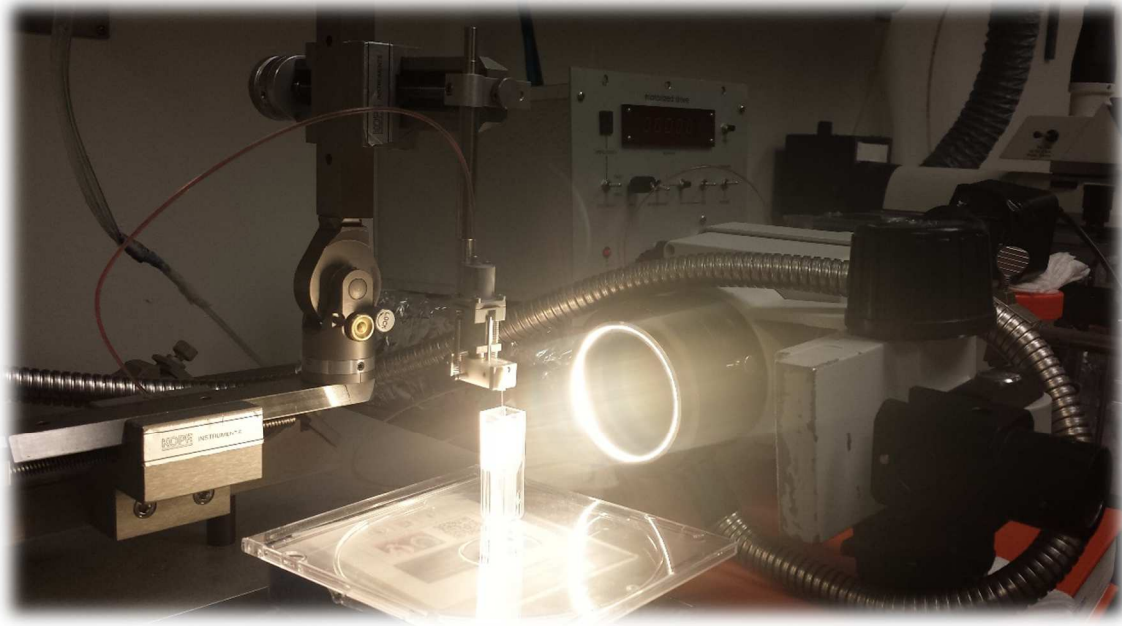


Figure 21 Experimental set up for strain distribution measurement

Experimental Protocol

To measure distribution of strain, we used one tungsten electrode connected to the hydraulic micromanipulator. Four different type of movement patterns were tested.

1: Unidirectional movement of 30 μm followed by 3 min IMI.

2: Bidirectional movement of 60 μm downward with 1 minute followed by 3 μm upward movement and 2 minutes IMI

3: Unidirectional movement of 20 μm followed by 40 sec IMI

4: Bidirectional movement of 60 μm downward followed by 40 μm upward and 20 sec IMI.

To measure strain distribution, we started recording when the electrode started to move 1mm inside the PDMS using a FHC (FHC Inc., Bowdoinham, ME) microdrive. Then we let the tissue to relax for 10 minutes and after that one of the above mentioned movement patterns were executed. Total of 4 videos were recorded.

Below are couple of the figures extracted from the videos for demonstration. First figure shows initial penetration and the second figure is a frame 30 seconds after that.

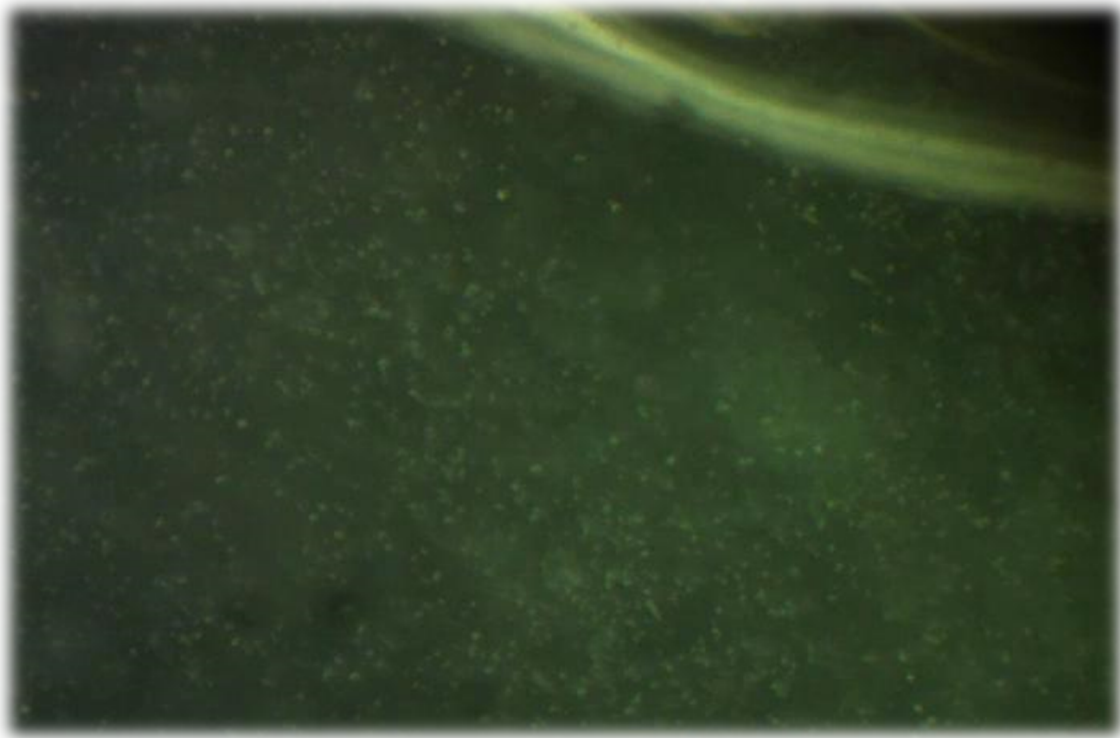


Figure 22: A frame from initial movement of electrode inside the PDMS. Microscale beads are shown as white dots



Figure 23 A frame after the initial penetration of electrode inside the PDMS.

Block Matching Algorithm

One of the most popular techniques for motion estimation is block matching algorithm.

The concept behind motion estimation is that the patterns corresponding to objects and background in a frame of video sequence move within the frame to form corresponding objects on the subsequent frame.

The idea behind block matching is to divide the current frame into a matrix of “macro blocks” that are then compared with the corresponding block and its adjacent neighbors in the previous frame to create a vector that stipulates the movement of the macro block from one location to another in the previous frame. This movement vector was calculated

for all the macro blocks in that frame. The search area for a macro block match is up to 'p' pixel on all four sides of the corresponding macroblock in previous frame. This 'p' is called search parameter. Larger motions needs larger p. The matching of one macro block with another is based on the result of Mean Absolute Difference (MAD). The macro block that result in the least cost is the one that matches the closest to current block.

$$MAD = 1/N^2 \sum \sum |C_{ij} - R_{ij}|$$

where N is the side of the macro block, C_{ij} and R_{ij} are the pixels being compared in current macro block and reference macro block, respectively.

In this research, we used block matching algorithm to find motion vectors from one frame to another frame. Time between two frames varied depending on the condition of the electrode (whether it is moving or it is stationary). For the first 10 second of the video, in which the microelectrode was moved 1mm inside the PDMS, we decided to compare the frames every 1 second. However, once the electrode stayed in place for 10 minutes to allow the tissue to relax, and the subsequent movement patterns were executed (unidirectional, bidirectional 30 μ m or unidirectional/ bidirectional 20 μ m). Below are there figures that show the motion vectors for three different conditions. Figure 24 represents the initial penetration of microelectrode inside the PDMS. As expected, there is significant movement right next to the electrode and almost zero movement on other regions. The two frames compared were 1 second apart from each other.

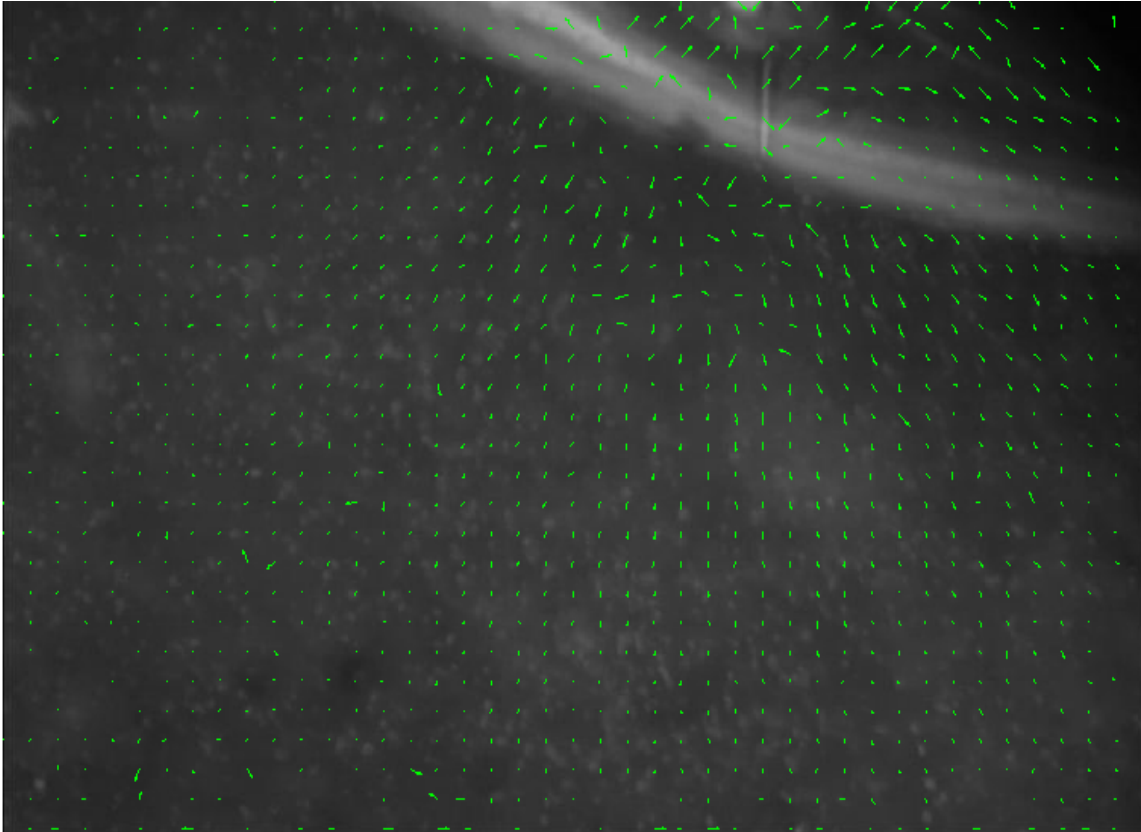


Figure 24 Motion vector for the initial penetration of electrode. Frames are one second apart.

Figure 25 shows the last two frames for the time the microelectrode reached 1mm inside the PDMS. We have compared two frames that are 1 second apart.

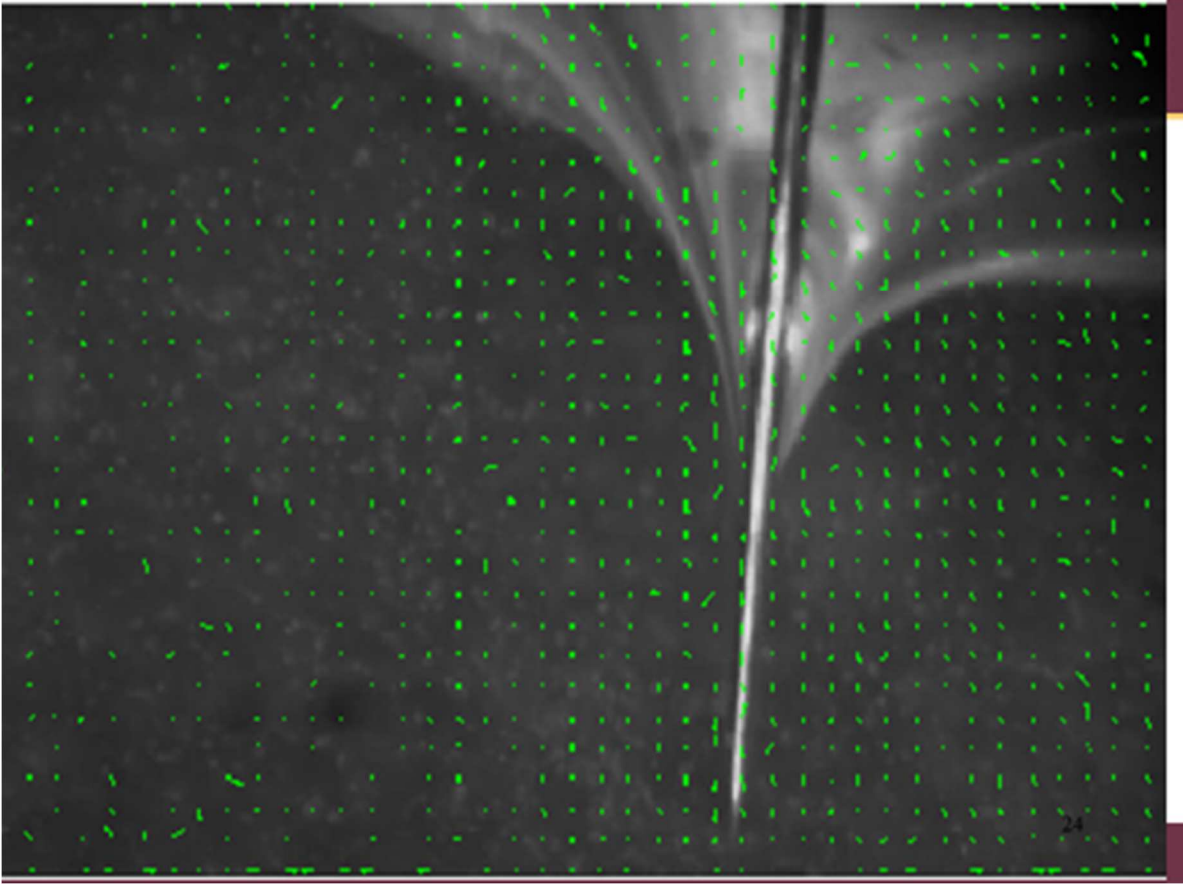


Figure 25: Motion vectors for the time microelectrode stopped movement, after 1mm penetration. Frames are one second apart.

In figure 25, movement of the particles along the microelectrode is clear. We still cannot see any motion vector further away from the electrode.

In figure 26, motion vectors for the end of the relaxation time period has been plotted. In this figure, time interval between two consecutive frames are two minutes. Since during

the relaxation time, movement of particles are extremely small and slow, we can see almost no movement in the motion vectors.

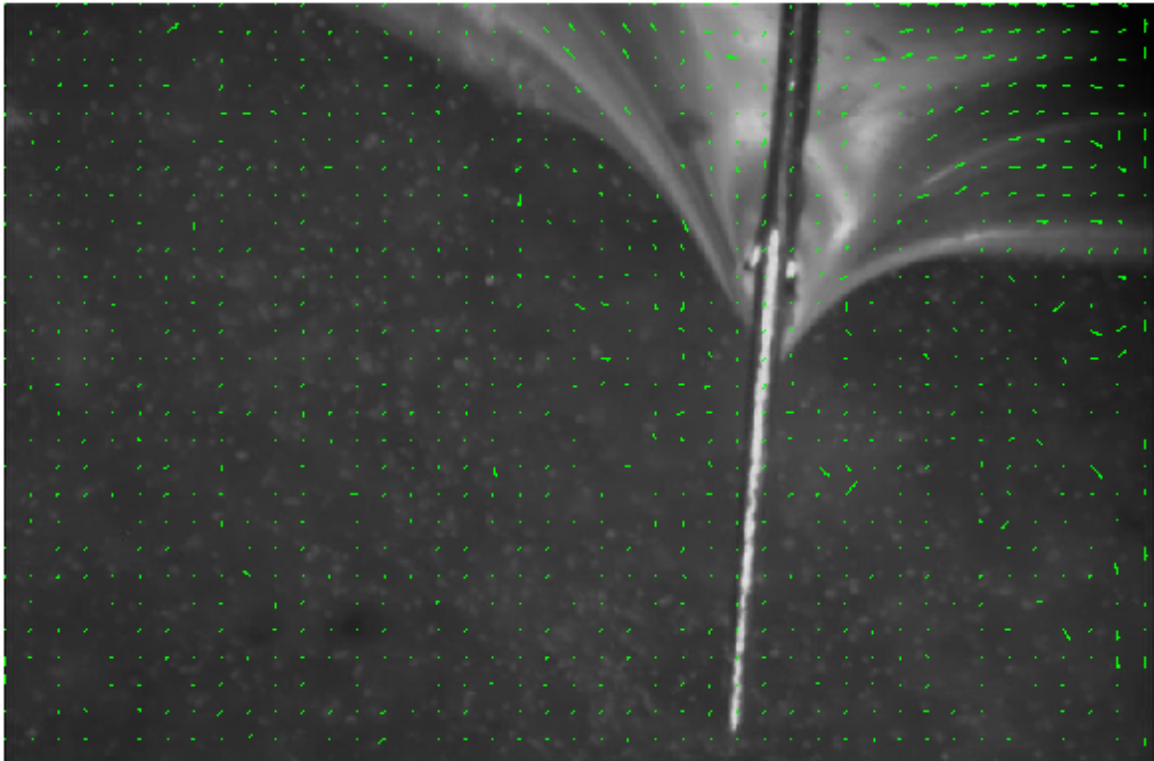


Figure 26: Motion vector for the end of the relaxation time. Frames are two minutes apart.

Tracking Single Particles

To measure strain distribution, in each experiment, we tracked 3 different particles in three different locations from the electrode. Particles were 200, 400, 700 μm away from the tip of the microelectrode. The rationale for choosing these distances was that we were interested to compare the strain measurements with the stress measurement reported in Chapter 2. The method we used to find Euclidean distance for a particle from a frame to frame was manual tracking. We developed a MATLAB code (refer to the appendix A) in which we were able to find the current position of the particle by clicking on it.

Results

Figure 27 shows displacement profile for unidirectional 30 μm downward movement of three different particles at locations 200, 400, 700 μm . As figure indicates, in the first 10 seconds of the video, electrode was moved 1 mm inside the PDMS. Thus, we see huge displacement of particles, up to 400 μm for this movement. Then, the tissue was left in place to relax for 10 minutes. After the relaxation period was done and particles reached steady state, the unidirectional 30 μm and 3 minutes IMI was started.

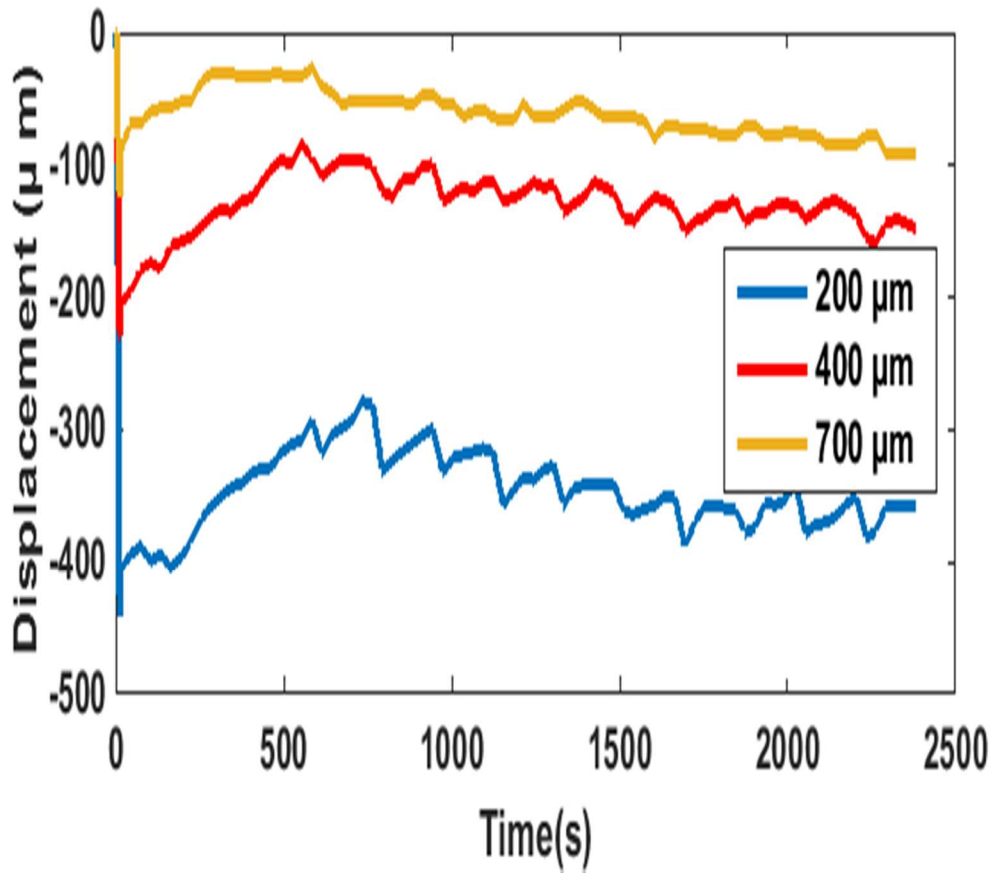


Figure 27: Strain measurement for unidirectional movement of 30 μm downward with 3 minutes IMI. Three different particles at three different locations from the tip of the microelectrode were evaluated

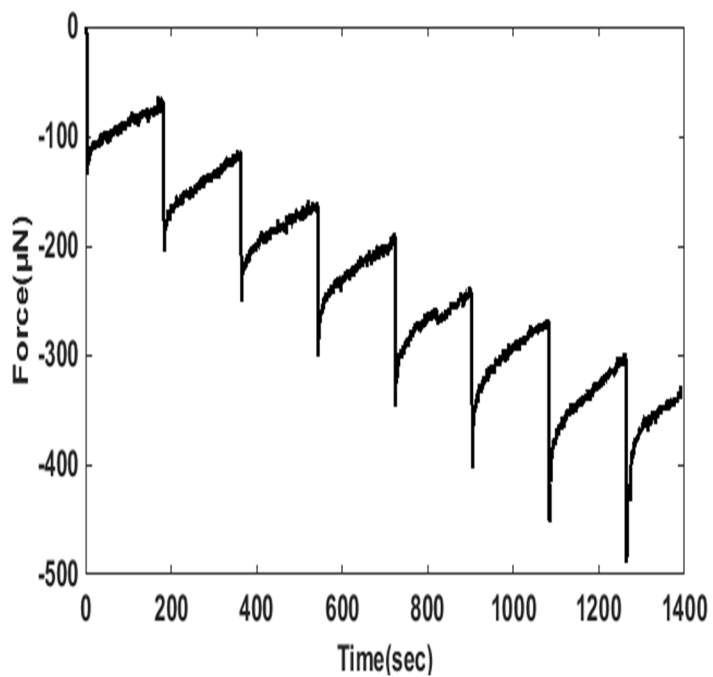


Figure 28: Corresponding force measurement for unidirectional 30 µm downward movement

As figure 28 indicates, for unidirectional movement of 30 µm, build up of stress is visible. As we expected, increase in displacement is observed in the microparticles as the microelectrode was moving 30 µm downward in each step.

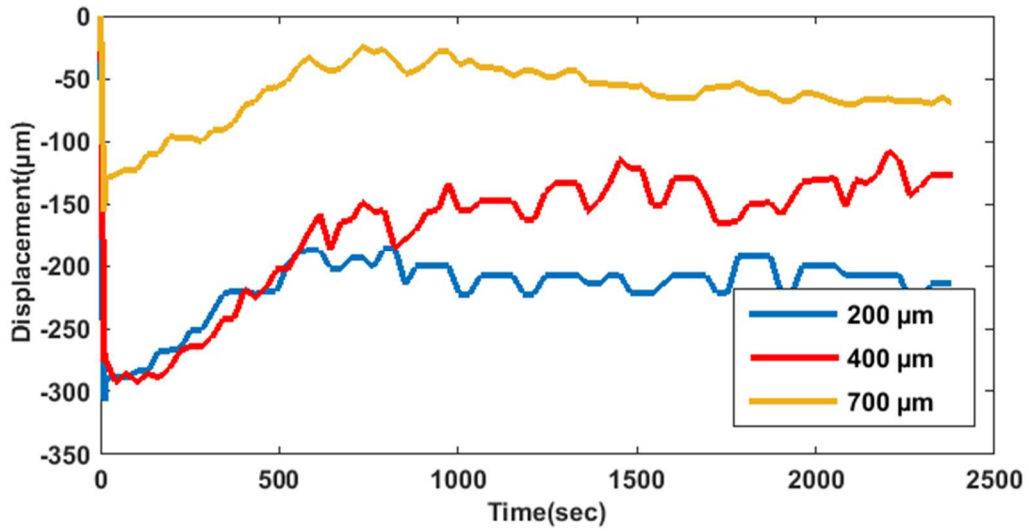


Figure 29: Strain measurement for bidirectional movement of $60\ \mu\text{m}$ downward with 1 minute IMI followed by $30\ \mu\text{m}$ upward with 2 minutes IMI. Three different particles at three different locations from the tip of the microelectrode were evaluated

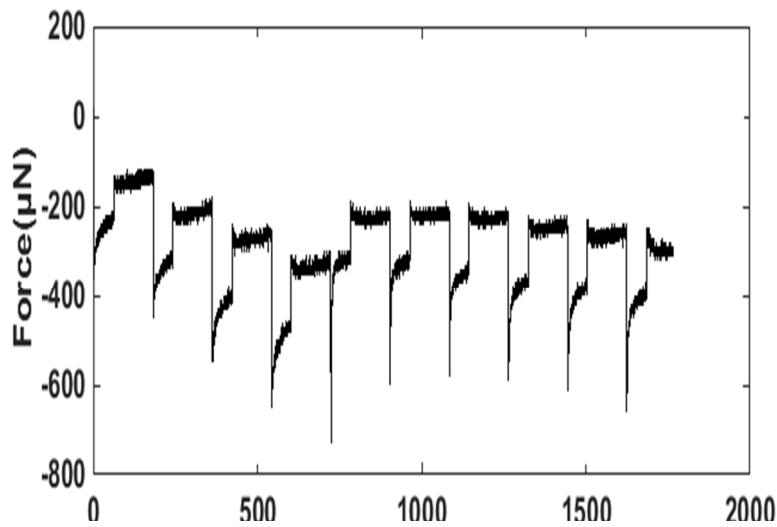


Figure 30: Corresponding force measurement for bidirectional $60\ \mu\text{m}$ downward movement with 1 minute IMI followed by $30\ \mu\text{m}$ upward movement with 2 minutes IMI

As figure 30 indicates, for bidirectional movement of $60\ \mu\text{m}$ downward followed by $30\ \mu\text{m}$ upward, quasi- steady state stresses is visible. From the strain measurement figure, figure 29, the quasi steady state for displacement of neurons is visible after the initial 1mm penetration. This is validating our initial hypothesis that bidirectional inchworm type movement will cause steady state of stress.

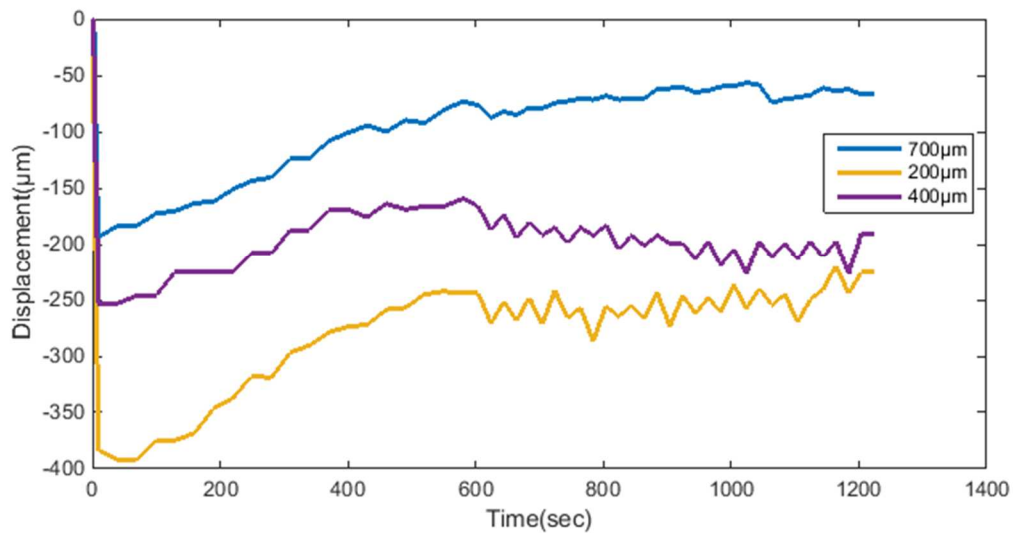


Figure 31: Strain measurement for bidirectional movement of $40\ \mu\text{m}$ downward with 20 seconds IMI followed by $20\ \mu\text{m}$ upward with 20 seconds IMI. Three different particles at three different locations from the tip of the microelectrode were evaluated

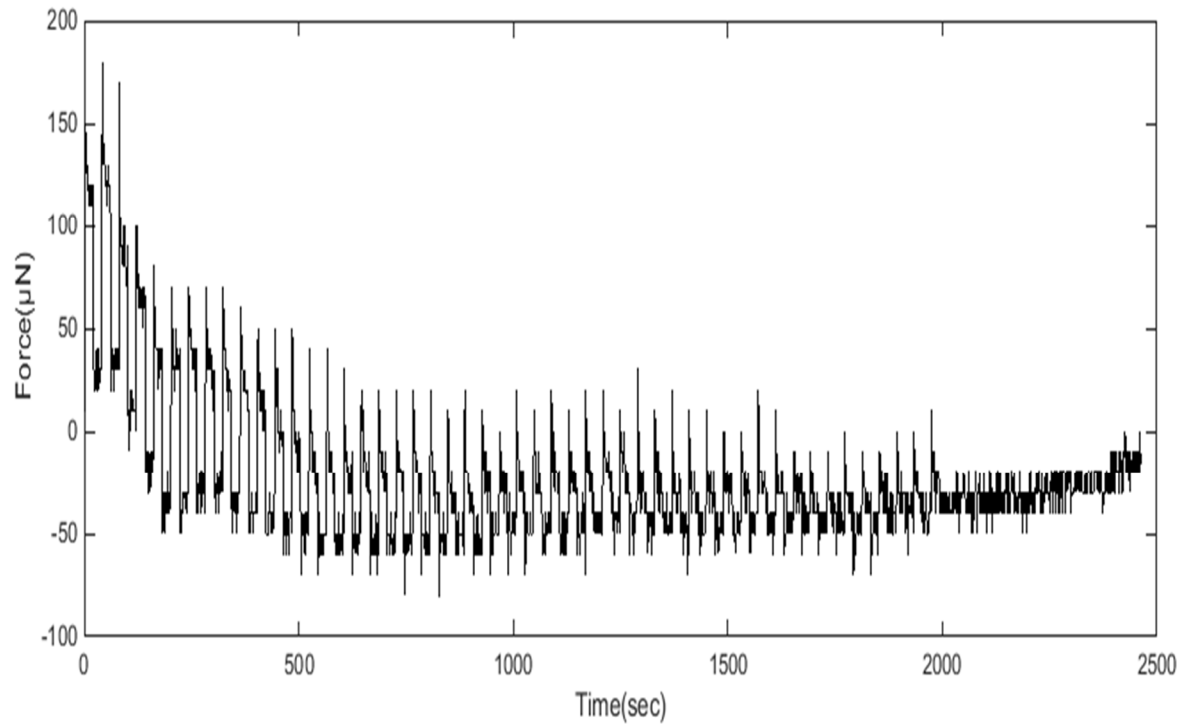


Figure 32: Corresponding force measurement for bidirectional 40µm downward movement with 20 seconds IMI followed by 20µm upward movement with 20 seconds IMI

As figure 32 indicates, for bidirectional movement of 40 µm downward followed by 20 µm upward, quasi- steady state stresses is visible. From the strain measurement figure, figure 30, the quasi steady state for displacement of neurons is visible after the initial 1mm penetration. This is validating our initial hypostasis that bidirectional inchworm type movement will cause steady state of stress.

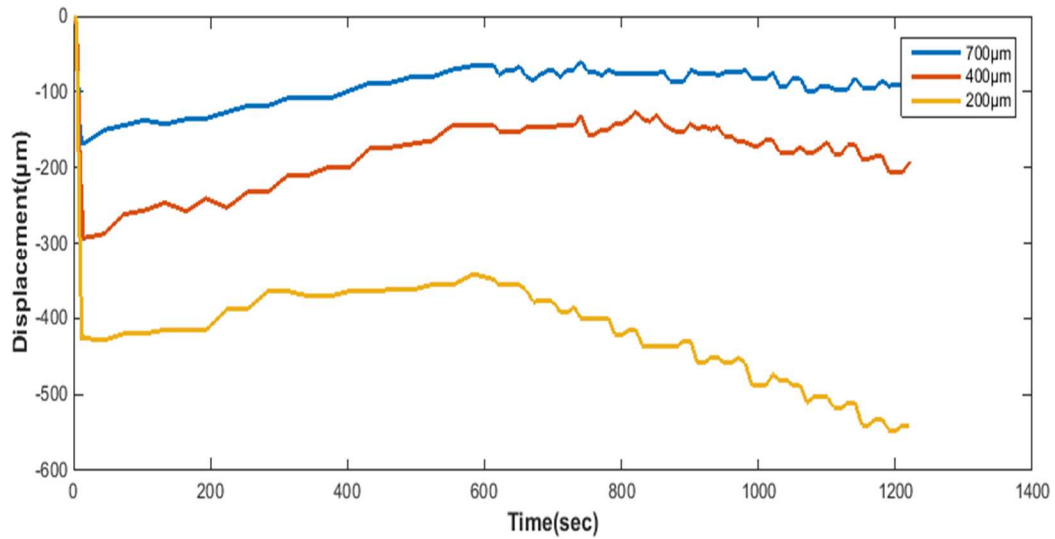


Figure 33: Strain measurement for unidirectional movement of 20 μm downward with 40 seconds IMI. Three different particles at three different locations from the tip of the microelectrode were evaluated

As figure 33 indicated, displacement of a particle is more when the particle is as close as 200 μm to the electrode. As the particle is further away from the electrode, the amount of displacement would decrease. For unidirectional movement pattern, build-up of stress is visible in figure 33.

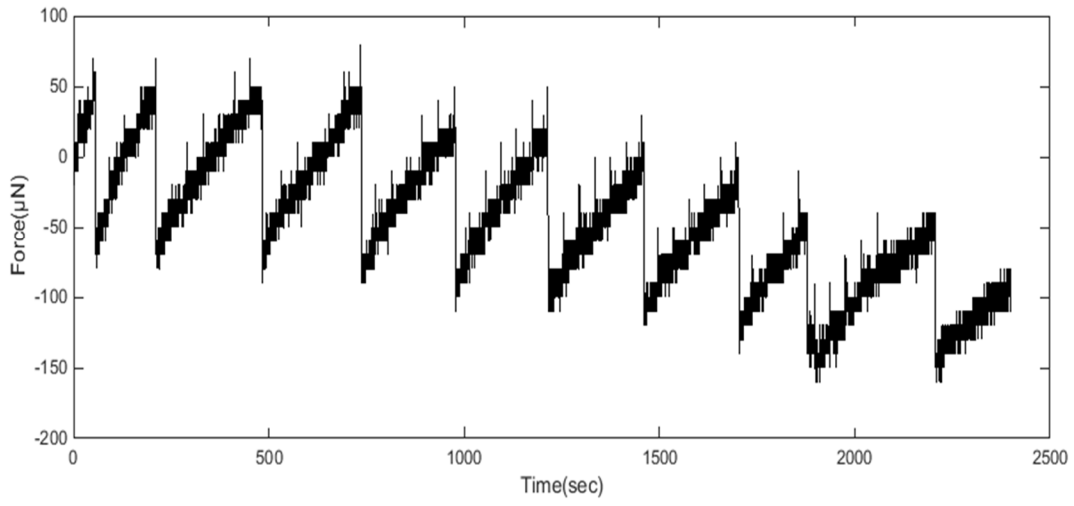


Figure 34: Corresponding force measurement for unidirectional 20 μm downward movement with 40 seconds IMI

Discussion

From stress measurement data, maximum shear stresses of up to 200 Pa were observed 500 microns away from a moving electrode, and up to 120 Pa were observed 1000 microns away from the moving micro electrode. Shear stresses appear to dissipate exponentially as a function of distance from the moving micro electrode. Besides, from stress curves, build up of stress for unidirectional movement pattern is visible. However, as expected, quasi-steady state stresses is distinctly visible during bidirectional movement.

From strain measurement, maximum displacements of up to 400 microns were observed for microparticles within 200 microns from the moving electrode, and up to 200 microns for microparticles within 400 microns from the moving electrode and up to 100 microns for microparticles within 700 microns from the moving electrode. Besides, displacements of microparticles are quasi-static in the case of micro electrodes moving bi-directionally in an inch-worm fashion, but steadily increase in the case of unidirectional micro electrode movement. The results from strain measurements significantly decreased displacement of microparticles under bidirectional movement of microelectrode.

REFERENCES

- 1: Vetter, Rio J., et al. "Chronic neural recording using silicon-substrate microelectrode arrays implanted in cerebral cortex." *Biomedical Engineering, IEEE Transactions on* 51.6 (2004): 896-904.
- 2: Engel, Andreas K., et al. "Invasive recordings from the human brain: clinical insights and beyond." *Nature Reviews Neuroscience* 6.1 (2005): 35-47.
- 3: Polikov, Vadim S., Patrick A. Tresco, and William M. Reichert. "Response of brain tissue to chronically implanted neural electrodes." *Journal of neuroscience methods* 148.1 (2005): 1-18.
- 4: Jackson, Nathan, et al. "Long-term neural recordings using MEMS based movable microelectrodes in the brain." *Frontiers in neuroengineering* 3 (2010).
- 5: Tolias, Andreas S., et al. "Recording chronically from the same neurons in awake, behaving primates." *Journal of neurophysiology* 98.6 (2007): 3780-3790.
- 6: Dickey, Adam S., et al. "Single-unit stability using chronically implanted multielectrode arrays." *Journal of neurophysiology* 102.2 (2009): 1331-1339.
- 7: Yamamoto, Jun, and Matthew A. Wilson. "Large-scale chronically implantable precision motorized microdrive array for freely behaving animals." *Journal of neurophysiology* 100.4 (2008): 2430-2440.
- 8: Jackson, Andrew, and Eberhard E. Fetz. "Compact movable microwire array for long-term chronic unit recording in cerebral cortex of primates." *Journal of neurophysiology* 98.5 (2007): 3109-3118.
- 9: Fee, Michale S., and Anthony Leonardo. "Miniature motorized microdrive and commutator system for chronic neural recording in small animals." *Journal of neuroscience methods* 112.2 (2001): 83-94.

- 10: Cham, Jorge G., et al. "Semi-chronic motorized microdrive and control algorithm for autonomously isolating and maintaining optimal extracellular action potentials." *Journal of Neurophysiology* 93.1 (2005): 570-579.
- 11: Wolf, Michael T., et al. "A robotic neural interface for autonomous positioning of extracellular recording electrodes." *The International Journal of Robotics Research* (2009).
- 12: Yang, Sungwook, et al. "Feedback controlled piezo-motor microdrive for accurate electrode positioning in chronic single unit recording in behaving mice." *Journal of neuroscience methods* 195.2 (2011): 117-127.
- 13: Kern, Thorsten A., et al. "A remotely controlled lightweight MRI compatible ultrasonic actuator for micrometer positioning of electrodes during neuroethological primate research." *Biomedical Engineering* 53.6 (2008): 292-299.
- 14: Christopher deCharms, R., David T. Blake, and Michael M. Merzenich. "A multielectrode implant device for the cerebral cortex." *Journal of neuroscience methods* 93.1 (1999): 27-35.
- 15: Sato, T., T. Suzuki, and K. Mabuchi. "A new multi-electrode array design for chronic neural recording, with independent and automatic hydraulic positioning." *Journal of neuroscience methods* 160.1 (2007): 45-51.
- 16: Szarowski, D. H., et al. "Brain responses to micro-machined silicon devices." *Brain research* 983.1 (2003): 23-35.
- 17: Stice, Paula, and Jit Muthuswamy. "Assessment of gliosis around moveable implants in the brain." *Journal of neural engineering* 6.4 (2009): 046004.
- 18: Britt, R. H., and G. T. Rossi. "Quantitative analysis of methods for reducing physiological brain pulsations." *Journal of neuroscience methods* 6.3 (1982): 219-229.
- 19: Chestek, Cindy, et al. "Neural prosthetic systems: current problems and future directions." *Engineering in Medicine and Biology Society, 2009. EMBC 2009. Annual International Conference of the IEEE. IEEE, 2009.*

- 20: Bragin, A., et al. "Multiple site silicon-based probes for chronic recordings in freely moving rats: implantation, recording and histological verification." *Journal of neuroscience methods* 98.1 (2000): 77-82.
- 21: Wilson, Fraser AW, et al. "A microelectrode drive for long term recording of neurons in freely moving and chaired monkeys." *Journal of neuroscience methods* 127.1 (2003): 49-61.
- 22: Suner, Selim, et al. "Reliability of signals from a chronically implanted, silicon-based electrode array in non-human primate primary motor cortex." *Neural Systems and Rehabilitation Engineering, IEEE Transactions on* 13.4 (2005): 524-541.
- 23: Liu, Xindong, et al. "Evaluation of the stability of intracortical microelectrode arrays." *Neural Systems and Rehabilitation Engineering, IEEE Transactions on* 14.1 (2006): 91-100.
- 24: Deadwyler, Sam A., et al. "A microdrive for use with glass or metal microelectrodes in recording from freely-moving rats." *Electroencephalography and clinical neurophysiology* 47.6 (1979): 752-754.
- 25: Andersen, R. A., et al. "Cognitive neural prosthetics." *Trends in cognitive sciences* 8.11 (2004): 486-493.
- 26: Taylor, Dawn M., Stephen I. Helms Tillery, and Andrew B. Schwartz. "Direct cortical control of 3D neuroprosthetic devices." *Science* 296.5574 (2002): 1829-1832.
- 27: Serruya, Mijail D., et al. "Brain-machine interface: Instant neural control of a movement signal." *Nature* 416.6877 (2002): 141-142.
- 28: Wessberg, Johan, et al. "Real-time prediction of hand trajectory by ensembles of cortical neurons in primates." *Nature* 408.6810 (2000): 361-365.
- 29: Patil, Parag G., and Dennis A. Turner. "The development of brain-machine interface neuroprosthetic devices." *Neurotherapeutics* 5.1 (2008): 137-146.
- 30: Branchaud, Edward, Joel W. Burdick, and Richard Andersen. "An algorithm for autonomous isolation of neurons in extracellular recordings." *Biomedical Robotics and Biomechatronics, 2006. BioRob 2006. The First IEEE/RAS-EMBS International Conference on*. IEEE, 2006.

APPENDIX A
MATLAB CODES

```
% Finding particle's location based on placing the cursor on it
```

```
clear; clc;
```

```
count=1;
```

```
for i=1:0.5:13
```

```
image=strcat('Uni-20-40',num2str(i),'.jpg');
```

```
pts(:,count) = readPoints(image);
```

```
time(count) = i;
```

```
count = count + 1;
```

```
end
```

```
for i=14:30:(10*60)+21
```

```
image=strcat('Uni-20-40',num2str(i),'.jpg')
```

```
pts(:,count) = readPoints(image)
```

```
time(count) = i;
```

```
count = count + 1;
```

```
end
```

```
for i=((10*60)+21:10:(20*60)+25)
```

```
image=strcat('Uni-20-40',num2str(i),'.jpg')
```

```
pts(:,count) = readPoints(image)
```

```
time(count) = i;
```

```
count = count + 1;
end
for i=1:107
    a(:,i)=(pts(:,i)-pts(:,1))*3.7
    b1=sqrt((a(1,:).^2)+(a(2,:).^2))
end
plot(time,-b1)
```

```
function pts = readPoints(image, n)
%readPoints  Read manually-defined points from image
% POINTS = READPOINTS(IMAGE) displays the image in the current figure,
% then records the position of each click of button 1 of the mouse in the
% figure, and stops when another button is clicked. The track of points
% is drawn as it goes along.

if nargin < 2
    n = Inf;
    pts = zeros(2, 0);
```

```

else

    pts = zeros(2, n);

end

imshow(image); % display image

xold = 0;

yold = 0;

k = 0;

hold on; % and keep it there while we plot

while 1

    [xi, yi, but] = ginput(1); % get a point

    if ~isequal(but, 1) % stop if not button 1

        break

    end

    k = k + 1;

    pts(1,k) = xi;

    pts(2,k) = yi;

    if xold

        plot([xold xi], [yold yi], 'go-'); % draw as we go
    end
end

```

```
else
    plot(xi, yi, 'go');    % first point on its own
```

```
end
```

```
if isequal(k, n)
```

```
    break
```

```
end
```

```
xold = xi;
```

```
yold = yi;
```

```
end
```

```
hold off;
```

```
if k < size(pts,2)
```

```
    pts = pts(:, 1:k);
```

```
end
```

```
end
```

```
% Code for extracting frames from video
```

```
clear;clc;
```

```
for k = ((10*60)+21:10:(20*60)+25) %fill in the appropriate number

vidObj = VideoReader('actual-pdms_20-40sec.wmv','CurrentTime',k);

vidObj.CurrentTime = k;

this_frame = readFrame(vidObj);

thisfig = figure();

thisax = axes('Parent', thisfig);

image(this_frame, 'Parent', thisax); title(thisax, sprintf('At time= %g second', k));

imwrite(this_frame, strcat('\Uni-20-40', num2str(k), '.jpg'), 'jpg')

end

close all
```